VOL. 2 No. 1
FEBRUARY 1960

UNIVERSITY OF CALIFORNIA
LIBRARY

RNAL OF THE

LESS-COMMON METALS

AN INTERNATIONAL JOURNAL ON
THEIR CHEMISTRY AND METALLURGY

RS:
UTHBERTSON (Nottingham)
BROTHER (Manchester)

RIAL ADVISORY BOARD:
RD (Paris)
CE COOK (Birmingham)
ROLY (Brussels)
INGHEUZIAN (Ottawa)
ETCHER (Harwell)
ONSER (Columbus, Ohio)
NSEN (Frankfurt a.M.)
DELLI (Genoa)
MM (Münster)
ROLL (Corvallis, Ore.)
RAY (Harwell)
WOTNY (Vienna)
IDGEON (Toronto)
OWELL (Wembley)
ALSTON (Hyattsville, Md.)
AN ARKEL (Leyden)
WORNER (Melbourne)
NTEMA (Menlo Park, Calif.)

ELSEVIER

GENERAL INFORMATION

Types of contributions

(a) Original research work not previously published in other periodicals.
(b) Reviews on recent developments in various fields.
(c) Short communications.
(d) Bibliographical notes and book reviews.

Languages

Papers will be published in English, French or German.

Submission of papers

Papers should be sent to one of the following Editors:

Professor J. W. CUTHBERTSON (*Metallurgy*), Department of Metallurgy, The University, University Park, Nottingham, England.
Professor F. FAIRBROTHER (*Chemistry*), The University of Manchester, Department of Chemistry, Manchester 13, England.

Authors should preferably submit two copies in double-spaced typing on pages of uniform size. Legends for figures should be typed on a separate page. The figures should be in a form suitable for reproduction, drawn in Indian ink on drawing paper or tracing paper, with lettering etc. in thin pencil. The sheets of drawing or tracing paper should preferably be of the same dimensions as those on which the article is typed. Photographs should be submitted as clear black and white prints on glossy paper.
All references should be given at the end of the paper. They should be numbered and the numbers should appear in the text at the appropriate places.
A summary of 50 to 200 words should be included. Authors of papers in French or German are encouraged to supply also a translation of the summary in English.

Reprints

Twenty-five reprints will be supplied free of charge. Additional reprints can be ordered at quoted prices. They must be ordered on order forms which are sent together with the proofs.

Publication

The *Journal of the Less-Common Metals* will have six issues to the volume, approx. 500 pages per volume.
Subscription price: £ 5.7.6 or $ 15.— or Dfl. 57.— per volume (post free).
For advertising rates apply to the publishers.

Subscriptions

Subscriptions should be sent to:

ELSEVIER PUBLISHING COMPANY, Spuistraat 110-112, Amsterdam-C., The Netherlands.

66 16808

5856-3/ TN1 J7 v.2

THE CONSTITUTION OF THORIUM–ZIRCONIUM ALLOYS CONTAINING MORE THAN 15% ZIRCONIUM AND THE EFFECT OF SOME THIRD ELEMENTS ON THE STABILITY OF THE BODY-CENTRED-CUBIC PHASE IN THESE ALLOYS

J. R. MURRAY*

Atomic Energy Research Establishment, Harwell, Berks. (Great Britain)

(Received January 6th, 1960)

SUMMARY

The constitution of thorium–zirconium alloys containing more than 15 at. % zirconium has been investigated, chiefly by metallographic methods. The decomposition of the high-temperature body-centred-cubic solid solution (β) has been found to be markedly affected by the purity of the starting materials. The β-phase in alloys prepared from commercial purity thorium and from "hafnium-free" zirconium or from zirconium containing 1 at. % hafnium has been found to break down to a $\beta_1 + \beta_2$ solid state miscibility gap which has a maximum at 52.5 at.% zirconium and a temperature of 950 ± 10°C. Such a miscibility gap has not been observed in alloys made from "iodide" thorium. Some observations on the metastable microstructures obtained by quenching from the β-field are also given, together with the crystal structures and lattice parameters of these alloys. The effect of additions of 2 at.% each of cerium, hafnium, indium, titanium and uranium on the decomposition of the β-field in alloys prepared from zirconium containing 1 at. % hafnium has also been studied. Indium, titanium and uranium increase the size of the miscibility gap, indium having the least effect and titanium the greatest. Additions of cerium and hafnium cause the gap to disappear, a smooth β-decomposition curve with a point of inflection in the composition range 45–55 at. % zirconium being obtained.

INTRODUCTION

A paper by CARLSON[1] indicated that zirconium was soluble in all proportions in the body-centred-cubic (β) modification of thorium and that this solid solution was not stable at room temperature. The shape of the boundary between the β-field and the two-phase region suggested that a $\beta_1 + \beta_2$ field might exist, although CARLSON obtained no direct evidence for this. A later paper by GIBSON, LOOMIS AND CARLSON[2] presented some high-temperature X-ray results to prove the existence of this $\beta_1 + \beta_2$ field and the author stated that "attempts at retaining a two-phase microstructure by quenching alloys from just above the [monotectoid] horizontal failed to yield evidence for such a loop".

In a recent survey of thorium phase diagrams, IVANOV AND BADAJEVA[3] confirmed the general aspects of CARLSON's diagram although they gave no information concerning the materials or experimental techniques employed.

* Now Mrs J. R. THOMSON at Metallurgy Department, Imperial College of Science and Technology, South Kensington, London.

The present results, on the occurrence of the $\beta_1 + \beta_2$ miscibility gap in alloys prepared from crystal bar and from production thorium, suggested that third elements might play an important role in affecting the stability of the body-centred-cubic phase. In an attempt to understand some of the factors governing this stability, alloys containing 2 at. % of each of Ce, Hf, In, Ti and U and 40–65 at. % zirconium containing 1 at. % hafnium were prepared and heat treated in the temperature range 910–1050°C. These alloying additions were chosen since each element was known to dissolve in thorium or zirconium in amounts greater than 15 at. %.

EXPERIMENTAL METHODS

Three grades of thorium were used, (a) bar stock material of 99.5–99.6% purity containing 400–700 p.p.m. carbon, 3000–4000 p.p.m. oxygen and total metallic impurities of less than 100 p.p.m., (b) electrolytic thorium with a carbon content of 100–150 p.p.m. and oxygen of 2000–3000 p.p.m., and (c) high-purity iodide material. Iodide zirconium containing 1 at. % hafnium was used for the main part of the work on the binary system and for the ternary alloys, while zirconium with less than 100 p.p.m. hafnium was used for a series of binary alloys containing 40–60 at. % zirconium.

All alloys were prepared by arc-melting in a zirconium-gettered argon atmosphere and, to keep segregation to a minimum, melts were confined to 20 g or less. Weight losses were negligible, chemical analysis results on a few early "buttons" agreed well with nominal compositions and later alloys were not analysed. For heat treatment, specimens were wrapped in tantalum or zirconium foil and sealed in silica capsules under a vacuum of better than 10^{-5} mm mercury or a low pressure (6–10 cm) of argon, depending on the annealing temperature.

Specimens were prepared for metallographic examination by conventional techniques using bakelite or cold-setting resin as the mounting medium and carborundum and diamond abrasives. The microstructure was revealed by several techniques:

(a) polish attack using γ-alumina as the abrasive and a very dilute HF solution;

(b) ionic bombardment in equipment which has been described by ARMSTRONG, MADSEN AND SYKES[4];

(c) electrolytic polishing in a solution containing 50 ml perchloric acid (60%), 175 ml glacial acetic acid and 100 ml ethylene glycol;

(d) etching in a solution of 10 parts by volume HF/90 parts by volume of a 60% wt./vol. $FeCl_3$ solution diluted as required;

Surfaces examined metallographically were, if necessary, subsequently investigated by X-ray methods using nickel-filtered copper radiation and a camera of 11.46 cm diam. in which the specimen could be continuously rotated and oscillated enabling a Debye-Scherrer pattern to be obtained.

Thermal analysis was performed *in vacuo*[5] using ThO_2 crucibles for melting-point determinations and hardness measurements were made with a standard Vickers diamond pyramid tester and a 20 kg load.

RESULTS

The general form of the thorium–zirconium diagram proposed by CARLSON using hafnium-free zirconium has been confirmed in the present work using zirconium

containing 1 at. % hafnium (Fig. 1). A sharp minimum in the solidus was found to occur at 1290° ± 10°C and 46 at. % zirconium, the transformation from β to α zirconium to be lowered to 650°C and the existence of a $\beta_1 + \beta_2$ field was observed

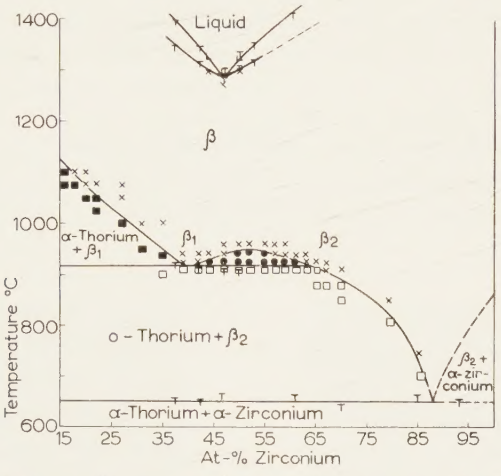

Fig. 1. Phase diagram of Th–Zr alloys containing more than 15 at. % Zr prepared from electrolytic or bar-stock Th and Hf-bearing Zr: ×, β solid solution; ●, $\beta_1 + \beta_2$; ■, $\alpha + \beta_1$; □, $\alpha + \beta_2$; L, showing liquation; T, thermal analysis result.

in alloys prepared with this zirconium and with "hafnium-free" zirconium. Metallographic evidence suggested that zirconium reacted with carbon present as an impurity in the thorium to form ZrC, since bright inclusions were observed in all alloys except those prepared from iodide thorium, in addition to the grey ThO_2 dendrites.

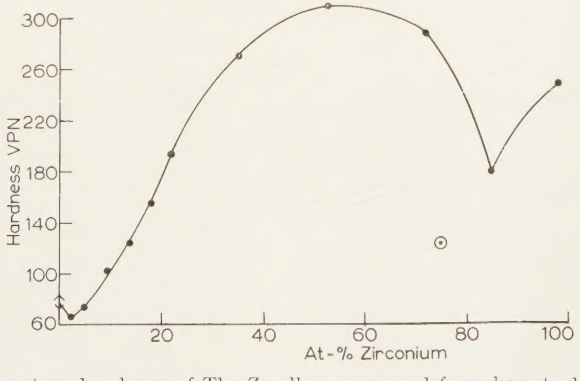

Fig. 2. Room temperature hardness of Th–Zr alloys prepared from bar-stock Th and quenched from 1000°C: ●, transformed on quenching; ◉, body-centred-cubic phase retained.

The results of a hardness survey on binary alloys quenched from 1000°C is shown in Fig. 2. The initial addition of zirconium caused a drop in hardness due to the removal of carbon as ZrC, further zirconium produced an increase in hardness to a

flat maximum of 280–310 VPN in the composition range 40–70 at. % zirconium, and a second hardness minimum occurred at the zirconium eutectoid composition of 85 at. % zirconium. These results are in agreement with those of CARLSON[1]. An alloy in which the body-centred-cubic phase was retained to room temperature had a lower hardness value than the specimens of neighbouring compositions which had transformed on quenching. Detailed results on various aspects of the system are described below.

Binary alloys quenched from the body-centred-cubic (β) field

The body-centred-cubic phase could only be retained by quenching to room temperature in alloys of a narrow range of composition close to 75 at. % zirconium and the

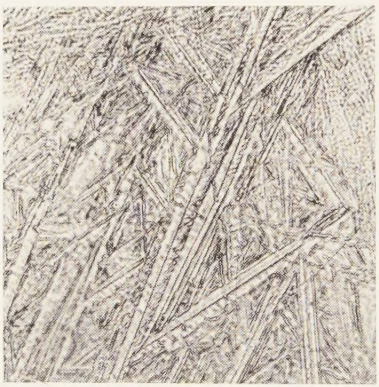

Fig. 3. Th–55 at. % Zr prepared from "iodide materials". Annealed 14 days 940°C, quenched, etched by ionic bombardment. Shows acicular structure (× 570).

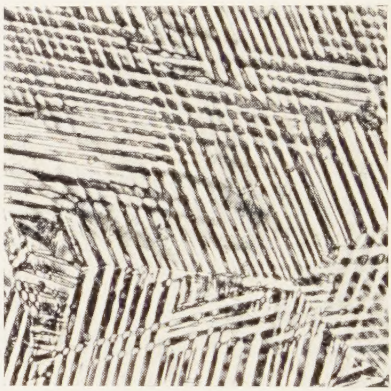

Fig. 4. Th–50 at. % Zr annealed 14 days 1000°C, quenched, etched by ionic bombardment. Polarised light. Showing "banded structure" (× 150).

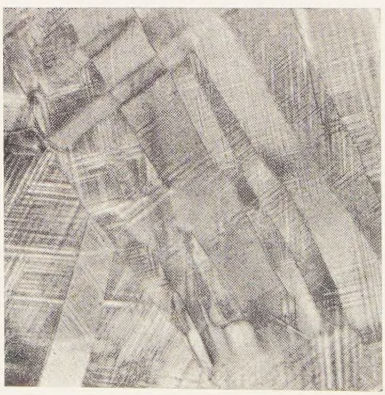

Fig. 5. Th–47 at. % Zr annealed 14 days 960°C, quenched, etched by ionic bombardment. Polarised light. Showing detail in "bands" (× 360).

Fig. 6. Th–47 at. % Zr annealed 1 day 1000°C, quenched, etched by ionic bombardment, centre of specimen (× 270).

room temperature lattice parameter of such an alloy was 3.71 Å. X-ray powder photographs obtained from the solid surfaces showed that alloys containing less zirconium transformed to a face-centred-cubic structure while those with more zirconium were hexagonal; in each case considerable line-broadening was observed, indicating that the lattices were strained. The microstructures depended on the purity of the material and on the rate of cooling; alloys prepared from iodide thorium and zirconium had an acicular appearance whether quenched into water or mercury (Fig. 3) while those made from commercial purity thorium frequently showed a "banded" structure (Fig. 4). At higher magnifications, the broad bands were seen to contain many smaller striations (Fig. 5). In some cases the "banded" structure occurred throughout the specimen, in others it was only observed near the edges, the centres having a "tweed-like" appearance (Fig. 6). The crystal structure and lattice parameter did not reflect this variation in the microsections.

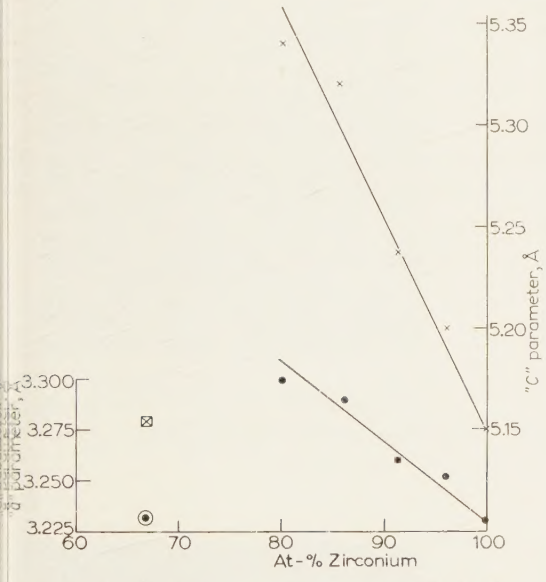

Fig. 7. Effect of Th concentration on α-Zr lattice parameters in quenched Zr-rich alloys: ●, "a" parameter, quenched from 1000°C; ×, "c" parameter, quenched from 1000°C; ◉, "a" parameter, quenched from 610°C; ⊠, "c" parameter, quenched from 610°C.

Fig. 8. Effect of Th on atomic volume of α-Zr in quenched alloys, assuming Vegard's law.

X-ray powder photographs from the polished surfaces of quenched alloys containing more than 75 at. % zirconium showed that the strain in the α-zirconium structure (as evidence by line broadening) increased with the thorium content. Approximate lattice parameter determinations revealed that the "a" and "c" parameters also increased with increase in thorium as illustrated in Fig. 7. If the atomic volume of the unit cell is plotted against composition it is found to be a good fit to a line representing the calculated change in atomic volume with composition, assuming Vegard's law to be obeyed (Fig. 8).

Equilibrium decomposition of the body-centred-cubic phase in binary alloys

These results are summarised in Fig. 1. Material which had been face-centred-cubic at the annealing temperature could be distinguished metallographically from that which had been body-centred-cubic, by its rapid tarnishing behaviour in the laboratory atmosphere. The quenched body-centred-cubic phase although transformed to a strained face-centred-cubic did not tarnish in air and the presence of the $\beta_1 + \beta_2$ field was difficult to distinguish unless the specimen was etched. Etching by $FeCl_3$/HF solution showed the structure in some specimens but the solution strength and etching time required varied so rapidly with composition, that etching by ionic bombardment was preferred since the necessary conditions did not change from specimen to specimen. Figs. 9–11 show the variation in the amounts of β_1 and β_2 present in a series of alloys

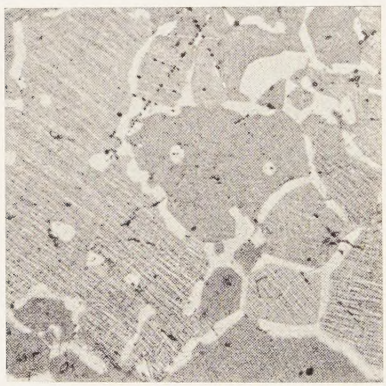

Fig. 9. Th–47 at. % Zr annealed 14 days 925°C, quenched, etched by ionic bombardment. Transformed β_1 (dark) + β_2 (light) (× 150).

Fig. 10. Th–54 at. % Zr annealed 14 days 925°C, quenched, etched by ionic bombardment. Transformed β_1 (dark) + β_2 (light) (× 150).

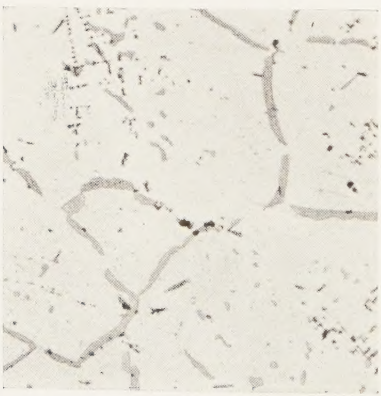

Fig. 11. Th–59 at. % Zr annealed 14 days 925°C, quenched, etched by ionic bombardment. Transformed β_1 (dark) + β_2 (light) (× 150).

Fig. 12. Th–52 at. % Zr annealed 28 days 940°C, quenched, etched by ionic bombardment. Transformed β_1 (dark) + β_2 (light) (× 150).

prepared from bar-stock thorium and zirconium containing 1 at. % hafnium and quenched from 925°C, while Fig. 12 shows the reduced contrast (due to lower composition differences between β_1 and β_2) at 940°C. The extent of the $\beta_1 + \beta_2$ field varied according to the purity of the starting materials (Fig. 13). In alloys prepared from hafnium-bearing zirconium the monotectoid horizontal occurred at 917.5 ± 7.5°C and the $\beta_1 + \beta_2$ miscibility gap extended from 38–65 at. % zirconium at this temperature, narrowing to 48–56 at. % zirconium at 940°C. The maximum of the loop *i.e.* the highest temperature at which the $\beta_1 + \beta_2$ field exists, occurred at approximately 950°C and 52.5 at. % zirconium. With hafnium-free alloys the temperature of the monotectoid horizontal and the maximum of the miscibility gap remained the same but the composition range was narrowed to approximately 46–58 at. % zirconium at the monotectoid temperature. No difference was observed between alloys prepared from "electrolytic" or bar-stock thorium but no evidence for the presence of a $\beta_1 + \beta_2$ field was observed in alloys of crystal bar thorium.

Alloys containing 37, 47, 61 and 67 at-% zirconium were homogenized at 1000°C for seven days, quenched to room temperature and subsequently annealed for six months at 610°C. X-ray photographs from the polished surfaces showed the presence of α-thorium $a = 5.082$ Å and α-zirconium $a = 3.24$ Å, $c = 5.16$ Å. Precipitation of α-thorium was observed along the edges of "bands" formed on quenching from 1000°C (Fig. 13); after attack polishing in a dilute HF solution, the matrix of each alloy responded to polarized light in a manner typical of α-zirconium.

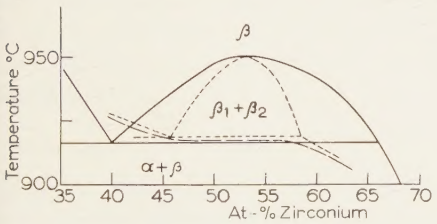

Fig. 13. Detail of β decomposition curve for binary Th–Zr alloys prepared from different purity starting materials. —— "Iodide" Th and "hafnium-bearing" Zr. – – – – Bar-stock Th and "hafnium-free" Zr. — — Bar-stock Th and "hafnium-bearing" Zr. *N.B.* Curves have been separated in the region of 917°C for clarity. There is no experimental evidence for such a separation.

Fig. 14. Th–47 at. % Zr annealed 7 days 1000°C, quenched then annealed 6 months 610°C. Showing precipitation of α-Th along edges of "bands" (× 150).

Ternary alloys

The metallographic results on the ternary alloys are summarized in Fig. 15. Each of the alloy additions reduced the temperature range over which the body-centred-cubic β-phase was stable. Indium, uranium and titanium increased the maximum temperature and area of the miscibility gap, titanium having the greatest effect and indium the least. With indium, the maximum of the loop remained at about 52.5 at. % zirconium, *i.e.* it moved to a lower thorium content, while with titanium it occurred

at the same thorium composition but with only 50 at. % zirconium. Additions of cerium and hafnium changed the shape of the β-field and lead to a smooth decomposition curve with a point of inflection at approximately 55 at. % zirconium. There were some indications that a three-phase (α-thorium + β_1 + β_2) region occurred in Th–Ce–Zr and Th–Hf–Zr alloys but the extent of such a field was not studied.

All specimens showed evidence of transformation on quenching, to structures akin to those observed in binary alloys. "Banded" and "tweed-like" microsections similar to Figs. 4 and 6 were noted in alloys quenched from the homogeneous β-field, while fine transformation markings occurred in the two-phase alloys similar to those shown in Figs. 9–12. All the alloys were bright and tarnish-resistant in air.

A hardness survey of ternary alloys quenched from the β-field showed that they had a similar hardness to the binary alloys with corresponding zirconium contents and a flat maximum of 300 ± 15 VPN over a range of 40–65 at. % zirconium.

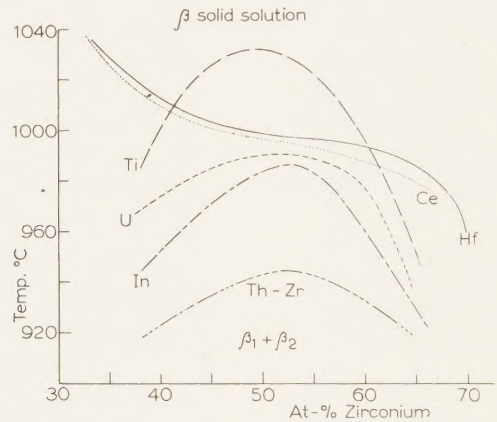

Fig. 15. Effect of 2 at. % of some ternary additions on the stability of the body-centred-cubic (β) phase in Th–Zr alloys prepared from bar-stock Th and "hafnium-bearing" Zr. — — — — binary Th–Zr, ... Th–Ce–Zr, —— Th–Hf–Zr, — — — Th–In–Zr, — — — — Th–Ti–Zr, — — — — Th–U–Zr.

DISCUSSION

Binary alloys

The form of the binary thorium–zirconium diagram shows general agreement with the work of GIBSON, LOOMIS AND CARLSON[2] who used hafnium-free zirconium and with IVANOV AND BADAJEVA[3] who do not state the purity of their materials. The zirconium used in the present binary alloys was either "hafnium-free" or contained 1 at. % hafnium, *i.e.* specimens whose composition lay within the miscibility gap contained approximately ½ at. % hafnium. The results on "hafnium-free" alloys confirm the work of GIBSON, LOOMIS AND CARLSON[2], while those from hafnium-bearing zirconium suggest that the width of the miscibility gap is increased by the addition of approximately ½ at. % hafnium although the maximum temperature of the $\beta_1 + \beta_2$ field is unaffected. One point of disagreement with GIBSON is in the ability to detect, by metallographic methods, the two body-centred-cubic phases when present together;

etching by ionic bombardment has been found to be a satisfactory method of revealing his structure. There is agreement with IVANOV AND BADAJEVA[3] on the monotectoid composition and temperature (assuming that they used "hafnium-bearing" zirconium) and on the fact that the body-centred-cubic phase may only be retained at room temperature by quenching alloys near 75 at. % zirconium. Assuming a linear variation of thermal expansion with composition in this system, the coefficient between room temperature and 1000°C for an alloy containing 75 at. % zirconium would be $9.0 \cdot 10^{-6}$ in./in./°C. From GIBSON's results[2] a lattice parameter of 3.72 Å would be expected at 1000°C for this alloy, in good agreement with the corrected value of 3.72 Å obtained here.

Since X-ray examination of several alloys annealed for six months at 610°C revealed only the presence of α-zirconium and α-thorium, it is concluded that no low-temperature ordered compound comparable with UZr_2 occurs in the thorium–zirconium system.

The occurrence of "banded microstructures" has been observed in several alloy systems notably indium–thallium[6,7] several manganese systems[8–10], uranium–titanium[11–13], uranium–titanium–zirconium[14], uranium–niobium[15], zirconium–hydrogen[16] and thorium–carbon[17], in each case a homogeneous phase at high temperatures has decomposed on quenching, to give such a structure. Where the crystallographic relationships of transformation have been determined, it has been shown that transformation has occurred by a double shear mechanism and it is therefore suggested that in the thorium-zirconium system, transformation by a similar mechanism occurs on quenching from the body-centred-cubic field. As far as is known, this is the first time that "banded" structures have been observed in thorium–zirconium alloys or as a result of a body-centred-cubic to face-centred-cubic transformation.

Ternary alloys

The pure metals, indium, uranium and titanium, like zirconium, have atomic diameters smaller than that of thorium and their effect on the size of the miscibility gap increases with increase in size-factor or lattice strain, *i.e.* titanium>uranium>indium. This is in accordance with the ideas put forward by HOWLETT[18] to explain the temperature and composition ranges of similar miscibility gaps which occur in several uranium alloy systems. IVANOV AND BADAJEVA[3] have reported briefly that additions of uranium to thorium–zirconium alloys cause the solid state miscibility gap to expand.

Equivalent amounts of cerium and hafnium have a more pronounced effect on the stability of the body-centred-cubic phase. The results on the two series of hafnium-bearing alloys suggest that small amounts of hafnium increase the width of the $\beta_1 + \beta_2$ field and that larger amounts raise the minimum temperature at which the body-centred-cubic phase is stable. Preliminary results on 2 at. % cerium alloys suggest that cerium might have a similar effect but alloys of intermediate compositions should be studied before definite conclusions can be reached.

It is of interest to note that 2 at. % of each of cerium, hafnium, indium, titanium and uranium will dissolve in the body-centred-cubic phase of thorium–zirconium alloys in the range 40–65 at. % zirconium although titanium will not dissolve in thorium.

ACKNOWLEDGEMENTS

The author would like to thank Mr. C. H. THOMAS for assistance with the preparation and heat treatment of the alloys, Mr. G. H. BANNISTER for assistance with thermal analysis and Messrs. R. H. JOHNSON and D. ARMSTRONG for assistance with etching by ionic bombardment. Thanks are also due to Dr. P. C. L. PFEIL and Dr. G. K. WILLIAMSON for encouragement and helpful discussions.

REFERENCES

1 O. N. CARLSON, *U.S. Atomic Energy Comm. Rept.* AECD 3206, 1950.
2 E. D. GIBSON, B. A. LOOMIS AND O. N. CARLSON, *Trans. Am. Soc. Metals*, 50 (1958).
3 O. S. IVANOV AND T. A. BADAJEVA, *Proc. Intern. Conf. Peaceful Uses Atomic Energy, Geneva*, 1958 A/CONF/15/P/2043.
4 D. ARMSTRONG, P. E. MADSEN AND E. C. SYKES, *Atomic Energy Research Establ. Rept.* M/R 2584, 1958.
5 S. J. LLOYD AND J. R. MURRAY, *J. Sci. Instr.*, 35 (1958) 252.
6 Z. S. BASINSKI AND J. W. CHRISTIAN, *Acta Met.*, 2 (1954) 101
7 Z. S. BASINSKI AND J. W. CHRISTIAN, *Acta Met.*, 4 (1956) 371.
8 S. J. CARLILE, J. W. CHRISTIAN AND W. HUME-ROTHERY, *J. Inst. Metals*, 76 (1949) 169.
9 Z. S. BASINSKI AND J. W. CHRISTIAN, *J. Inst. Metals*, 80 (1952) 659.
10 V. GRIFFITHS AND H. O'NEILL, *J. Inst. Metals*, 85 (1956) 81.
11 A. G. KNAPTON, *J. Inst. Metals*, 83 (1955) 497.
12 A. G. HARDING AND M. B. WALDRON, *Atomic Energy Research Establ. Rept.* M/R 2673, 1958.
13 A. G. HARDING, M. B. WALDRON AND C. KNIGHT, *Atomic Energy Research Establ. Rept* M/R 2673A, 1958.
14 B. HOWLETT, Private communication.
15 P. C. L. PFEIL, J. D. BROWNE AND G. K. WILLIAMSON, *J. Inst. Metals*, 87 (1958–59) 204.
16 D. WHITWHAM, M. A. HUBER AND J. HERENGUEL, *Acta. Met.*, 7 (1959) 65.
17 P. CHIOTTI, *U.S. Atomic Energy Comm. Rept.* AECD 3072, 1950.
18 B. HOWLETT, *Associated Electrical Industries Research Rept.* A. 890, 1959.

ORDERING IN CoPt-NiPt ALLOYS

J. C. WOOLLEY AND B. BATES

Department of Physics, University of Nottingham (Great Britain)

(Received January 28th, 1960)

SUMMARY

The effects of ordering in alloys of Co–Ni–Pt which belong to the pseudo-binary system CoPt–NiPt have been studied as an initial step in the investigation of their possible permanent magnet properties. Six alloys having equal increments of composition have been investigated, and the lattice parameter values for both ordered and disordered structures determined. X-ray techniques have been used to estimate the ordering temperatures, and the type of ordering reaction (continuous or discontinuous) occurring at various temperatures has been investigated. Possible values of percentage disregistry between the ordered and disordered structures have been calculated. The influence of the measured parameters on the possible production of hard magnetic materials from these alloys is briefly discussed.

INTRODUCTION

In a recent paper[1] an X-ray investigation of the ordering occurring in ternary alloys of the system CoPt–FePt has been discussed, with particular reference to those properties which are of interest when the possible magnetic behaviour of the alloys is being considered. In addition to the measurement of lattice parameter values for both disordered and ordered alloys, the variation of ordering temperature with composition was determined and an investigation was made of the nature and rate of development of the ordered phase at various compositions and temperatures. Information of this type has proved of interest in the case of the binary alloy CoPt in so far as development of permanent magnet properties is concerned.

A second series of alloys which should show similar properties are the CoPt–NiPt alloys. Previous work[2] has indicated that both CoPt and NiPt show the normal AuCu type ordering. The effects in CoPt have already been discussed in some detail[1] and will not be repeated here. Little work has been carried out on the Ni–Pt alloys. ESCH AND SCHNEIDER[3] reported that in the equiatomic alloy NiPt the transformation from disordered cubic to ordered tetragonal structure occurs at about 645°C, and that the lattice parameters of the ordered structure are $a_0 = 3.823$ Å and $c/a = 0.939$. The Curie temperature in the disordered Ni–Pt alloys drops rapidly from 358°C for pure nickel, reaching room temperature at 30 at. % platinum and tending to absolute zero at about 60 at. % platinum. Thus, the Curie temperature of NiPt is very low and this alloy shows no ferromagnetism at room temperature. Because of this, the nickel-rich alloys of the CoPt–NiPt system are likely to be of less interest from the magnetic viewpoint but the cobalt-rich alloys could still be of considerable tech-

nological interest. The whole system is of interest from a study of ordering mechanisms etc., and the work described here forms the initial stage in an investigation of the same ordering properties as have been described for the CoPt–FePt system.

ALLOYS AND METHODS OF MEASUREMENT

The alloys used for this work were provided by the Mond Nickel Co. Ltd. The nominal compositions were chosen to cover the range from CoPt to NiPt in intervals of 10 at. %, *i.e.*, (i) 10 at. % Ni, 40 at. % Co, 50 at. % Pt, (ii) 20 at. % Ni, 30 at. % Co, 50 at. % Pt, etc. The alloys were made by argon-arc melting, were homogenised, and then machined into bars 3 cm long and 7 mm square, suitable for magnetic work. Specimens cut from each bar were analysed and the results of the analyses are given in Table I.

TABLE I

COMPOSITION OF ALLOYS

Alloy	*Wt. % Ni*	*At. % Ni*	*Wt. % Co*	*At. % Co*	*Wt. % Co*	*At. % Pt*
A	23.1	49.96	—	—	76.9	50.04
B	18.5	39.97	4.7	10.11	76.8	49.92
C	14.3	30.90	8.9	19.15	76.8	49.94
D*	9.2	19.99	13.7	29.65	76.8	50.22
E	4.7	10.12	18.8	40.31	76.5	49.57

* Specimen D contained 0.14 at. % tungsten.

The techniques used for the treatment and measurement of these alloys were identical with those described for the CoPt–FePt alloys[1]. Roughly cylindrical specimens, approximately 1 cm long and 0.4 mm diam. were cut from the alloy ingots and used for X-ray powder photograph measurements after various suitable heat treatments. The difficulties in obtaining a disordered specimen experienced with the iron-rich alloys of the CoPt–FePt system because of the high ordering temperatures were not present in this case as all ordering temperatures were found to be below 820°C.

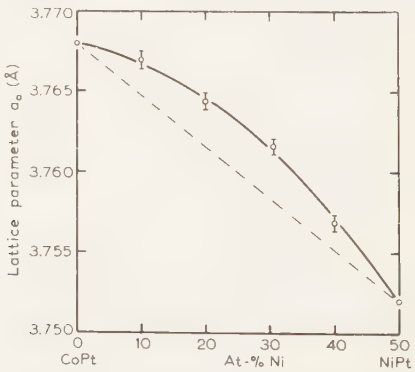

Fig. 1. Variation of lattice parameter a_0 as a function of composition for disordered alloys.

RESULTS AND DISCUSSION

To obtain the disordered condition, specimens of all alloys were heated for approximately 1 h at 1000°C and then quenched in water. X-ray photographs were obtained with a precalibrated 19 cm powder camera and Cu Kα radiation and values of the cubic lattice parameter a_o determined. The variation of a_o as a function of at. % nickel present in the alloy is shown in Fig. 1, and the accuracy of these parameters is estimated to be better than ± 0.001 Å. It is seen that Vegard's Law is not satisfied, the experimental results showing a maximum deviation from the Vegard line of approximately 0.003 Å in a lattice parameter of 3.763 Å.

To produce ordering in the alloys for lattice parameter measurements, specimens of each alloy were annealed under suitable conditions, and then slowly cooled to room temperature to avoid strains in the material. The temperature and time of annealing required to ensure that complete ordering was obtained were determined from the investigation of the ordering reaction described later. The times and temperatures used were as follows: alloys E and F (CoPt) 6 days at 650°C, alloys B, C and D 3 days at 600°C, and alloy A (NiPt) 18 days at 550°C. The results obtained with the ordered specimens are shown in Fig. 2. In all cases an ordered face-centred tetragonal structure is obtained similar to that for CoPt and NiPt, and values of a_o and c/a are plotted as a function of at. % nickel in the alloy. The accuracy of the a_o value is estimated to be ± 0.001 Å and that of c/a to be ± 0.001.

The difficulties experienced in the case of the CoPt–FePt alloys[1] due to the deviation of the at. % platinum from a value of 50% are much less important in this case, for, as is seen from Table I, the maximum deviation of platinum content from 50 at. % is 0.43 at. % in the case of alloy E, and therefore it is considered that the results in Figs. 1 and 2 are reasonably representative of the 50 at. % platinum alloys.

From Fig. 2 it is seen that again the a_o *vs.* composition curve does not follow a Vegard line, but in this case intersects that line at 25 at. % nickel, *i.e.* at the compo-

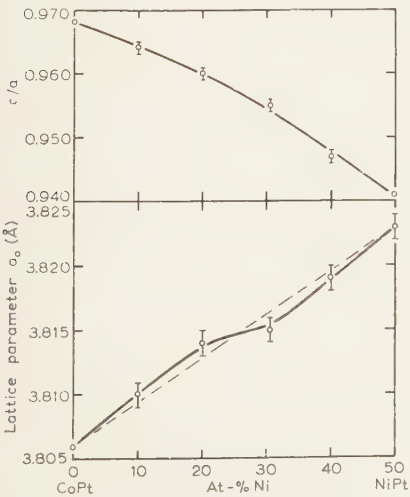

Fig. 2. Variation of lattice parameter a_o and ratio c/a as a function of composition for ordered alloys.

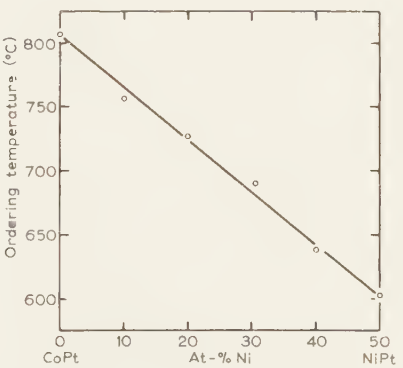

Fig. 3. Variation of ordering temperature as a function of composition.

sition with equal at. % of cobalt and nickel. APTEKAR AND FINKELSTEIN[4] have shown from thermodynamical considerations that this type of curve indicates a tendency for the system to develop either a closed miscibility gap or ordering, centred on the composition at which the intersection occurs. Neither of these effects were observed experimentally, but if extra ordering were to occur it would not have been observed with the X-ray techniques used here. This is because the ordering indicated by the lattice parameter results would be in addition to the normal platinum and cobalt-nickel layering of the AuCu structure, and would be an ordering of cobalt and nickel atoms in those (001) planes of the tetragonal structure which are occupied by these atoms. Owing to the very close values of the X-ray scattering factors of cobalt and nickel, ordering between these atoms would be detected only with considerable difficulty by X-ray techniques.

Measurements were made to determine the ordering temperature for each alloy by the method of annealing at various temperatures and quenching, as used for the CoPt–FePt alloys. Fig. 3 shows the values of ordering temperature determined in this way, the accuracy of the temperature values being estimated as approximately ± 5°C. The graph shows a practically linear decrease of ordering temperature with nickel content. The temperature value observed for NiPt is 603°C, which is rather lower than the approximate figure of 645°C given by ESCH AND SCHNEIDER[3].

Investigations were also carried out to determine the types of ordering reaction occurring in the various alloys. In each case the variation of the profile of the 311 and 113 lines of the X-ray powder photograph was observed for various times of anneal at various chosen temperatures. The two types of reaction to be expected are illustrated by the results for CoPt specimens annealed at 500°C and 700°C respectively. These curves were discussed in the CoPt–FePt work and for clarity are repeated here in Fig. 4. The results at 500°C, shown in Fig. 4a, are typical of a discontinuous reaction, while in Fig. 4b, the results at 700°C show typical continuous reaction profiles.

Similar observations were made on the alloys of the ternary system. In the case of alloy A (NiPt itself) and alloy B (containing 40 at. % of nickel) it was found that

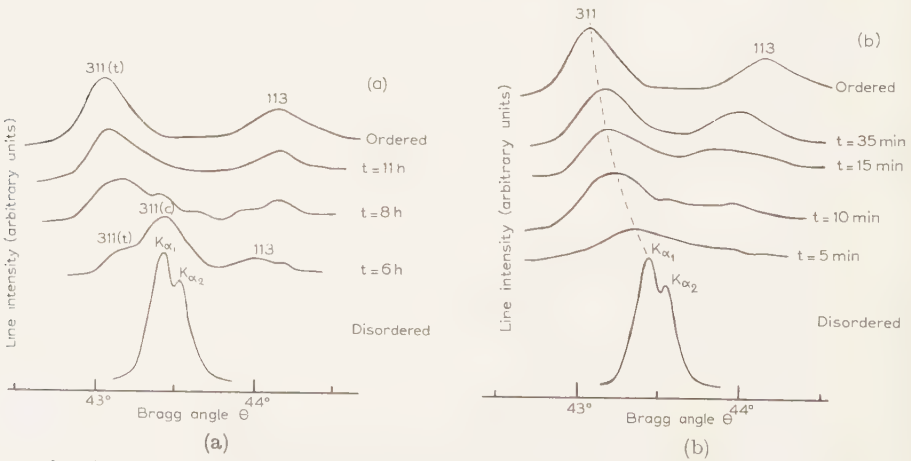

Fig. 4. Profiles of 311 and 113 lines for alloy F (nominal 50 Co, 50 Pt) after various annealing treatments (t = time of anneal). (a) Annealed at 500°C. (b) Annealed at 700°C.

nnealing at 500°C gave the high temperature continuous reaction and the appropri- te line profiles and annealing times are shown in Figs. 5 and 6. The rate of reaction was rather slower than in the case of CoPt, and longer anneals were required to give n ordered structure. No attempts were made with these two alloys to detect a discontinuous reaction at lower temperatures because of the very long annealing times which would have been required.

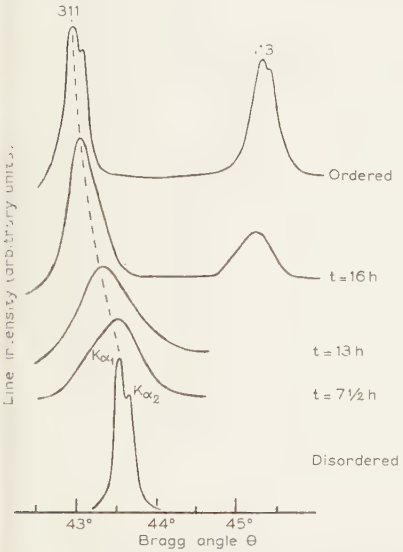

Fig. 5. Profiles of 311 and 113 lines for alloy A (nominal 50 Ni, 50 Pt) after annealing at 500°C (t = time of anneal).

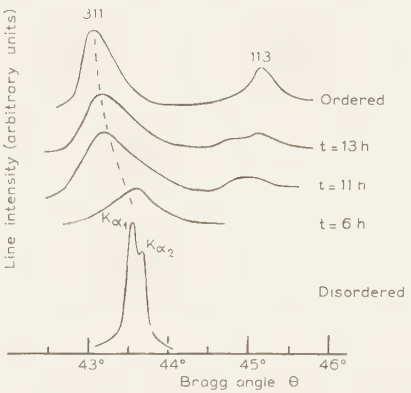

Fig. 6. Profiles of 311 and 113 lines for alloy B (nominal 10 Co, 40 Ni, 50 Pt) after annealing at 500°C (t = time of anneal).

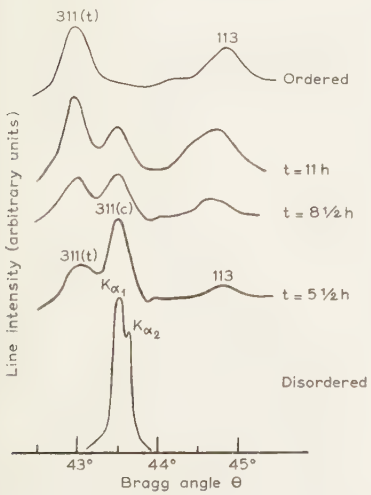

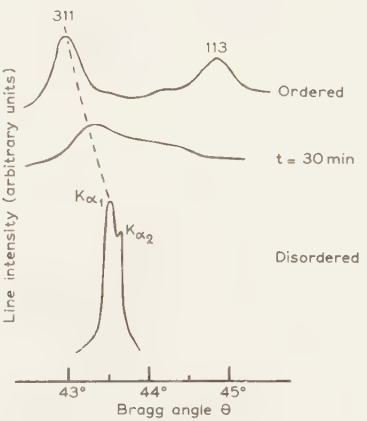

Fig. 7. Profiles of 311 and 113 lines for alloy C (nominal 20 Co, 30 Ni, 50 Pt) after various annealing treatments (t = time of anneal). (a) Annealed at 500°C. (b) Annealed at 650°C.

The alloys C, D and E (containing 30, 20 and 10 at. % nickel respectively) were found to show a discontinuous reaction when annealed at 500°C, and the appropriate line profiles and annealing times are shown in Figs. 7a, 8a, and 9a, respectively. Since the ordering temperature of these alloys falls with increased nickel content (Fig. 3), it was necessary in some cases to anneal at a temperature other than 700°C to observe the continuous reaction, and it was decided to anneal in each case at approximately 50°C below the ordering temperature. Thus, alloy C was annealed at 650°C, D at 675°C, and E at 700°C. In each case a continuous reaction was observed and the appropriate line profiles and annealing times are shown in Figs. 7b, 8b and 9b. In these cases, the increase in temperature gives more rapid reaction rates than those

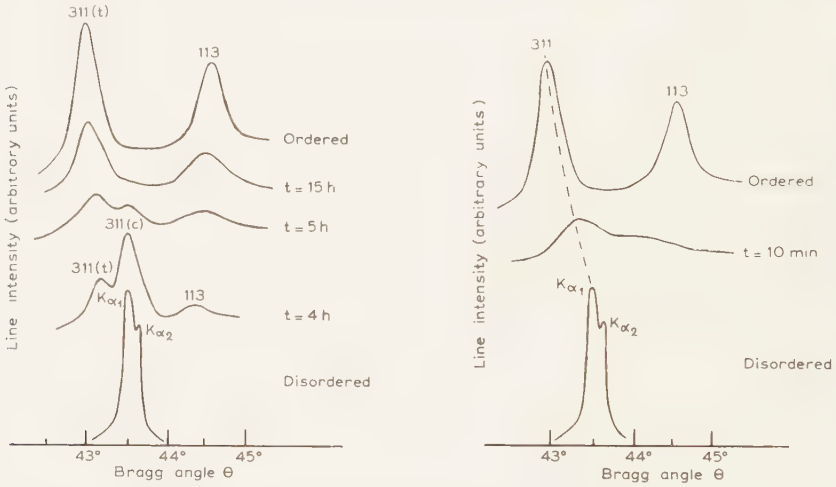

Fig. 8. Profiles of 311 and 113 lines for alloy D (nominal 30 Co, 20 Ni, 50 Pt) after various annealing treatments (t = time of anneal). (a) Annealed at 500°C. (b) Annealed at 675°C.

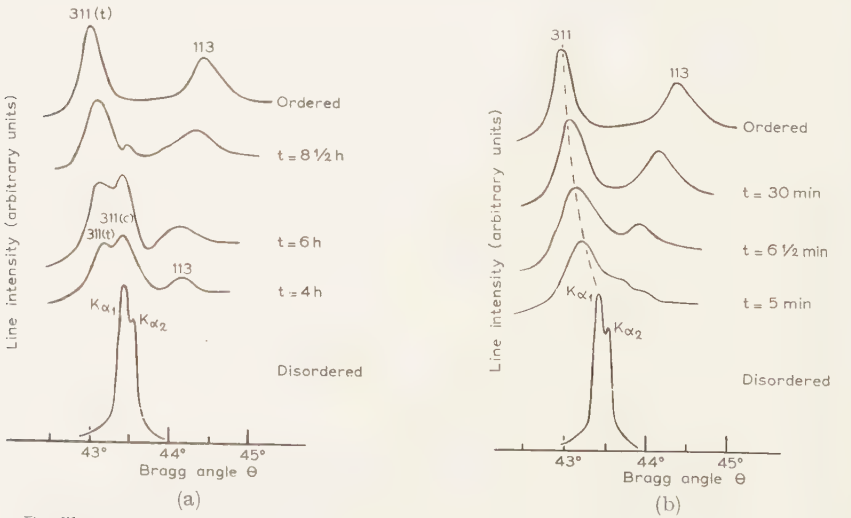

Fig. 9. Profiles of 311 and 113 lines for alloy E (nominal 40 Co, 10 Ni, 50 Pt) after various annealing treatments (t = time of anneal). (a) Annealed at 500°C. (b) Annealed at 700°C.

or the discontinuous reactions, and so only a limited number of intermediate line profiles have been obtained.

In general, the types of ordering reaction observed for CoPt are found to occur also in the ternary alloys. Owing to the larger lattice tetragonality, and therefore resolution of cubic and tetragonal lines, in this system, there is little doubt that the higher temperature ordering reaction is a continuous process and is not line broadening associated with lack of line resolution, as suggested by HARDY AND HEAL[5]. The temperature of transition from continuous to discontinuous reaction decreases with increased nickel content, and although no quantitative measurements of the variation in the rate of ordering with composition have been made, the results show that with increased nickel content the rate of ordering reaction is reduced.

Although no information has been obtained as to the actual cohabiting planes of the ordered and disordered structures, from the lattice parameter values given in Figs. 1 and 2 calculations can be made for the various alloys of the possible percentage disregistry for various combinations of planes. As was shown by NEWKIRK *et al.*[6] in the case of CoPt, the two combinations giving small disregistry values are (110) disordered: (101) ordered and (111) disordered: (111) ordered. Table II gives the percentage disregistry ($\Delta A/A$ expressed as a percentage) for these two combinations for the six alloys investigated. It is seen that as in the case of the CoPt–FePt alloys, the (111) disordered: (111) ordered combination gives the smallest percentage disregistry in every case.

TABLE II

PERCENTAGE DISREGISTRY CALCULATED FROM LATTICE PARAMETER VALUES

Alloy	*Nominal at. % composition*	*Percentage disregistry*	
		$(110)_{dis.}$: $(101)_{ord.}$	$(111)_{dis.}$: $(111)_{ord.}$
A	50Ni 50Pt	0.85	—0.25
B	10Co 40Ni 50Pt	0.65	—0.25
C	20Co 30Ni 50Pt	0.65	—0.25
D	30Co 20Ni 50Pt	0.60	—0.08
E	40Co 10Ni 50Pt	0.65	0
F	50Co 50Pt	0.41	—0.14

Sign of disregistry given by $\Delta A = \text{Area}_{\text{ordered}} - \text{Area}_{\text{disordered}}$.

CONCLUSIONS

The above results show that the ordering which occurs in CoPt and NiPt and which is responsible for the hard magnetic behaviour of the former material, also occurs throughout the whole range of composition of the CoPt–NiPt alloys. Thus, similar magnetic properties are to be expected for those ternary alloys in which the Curie temperature has a sufficiently high value. No measurements have as yet been made for these alloys of the variation of Curie temperature with composition, but this can be expected to fall as the nickel content is increased, and thus the alloys likely to be of greater interest from the technological point of view are those of higher cobalt content. For these alloys, the variation with composition of the calculated disregistry values is relatively small, bearing in mind the inaccuracy in the determination of this small quantity from the experimental values of the lattice parameters. Although the ordering temperature falls as the nickel content increases over the range of alloys

which are of interest magnetically, this effect is relatively small and the continuous ordering reaction can be obtained at such temperatures and resultant rates of ordering as to allow a reasonable control of the degree of development to be obtained by normal annealing techniques. Thus development of hard magnetic properties should be quite feasible for the alloys of smaller nickel content, and a programme of work to investigate these properties is being carried out.

ACKNOWLEDGEMENTS

We are indebted to Professor L. F. BATES for the facilities of his laboratory and to Dr. M. E. HAINE of Messrs. Siemens Edison Swan Ltd. for a maintenance grant to one of us (B.B.). We also wish to thank the Mond Nickel Co. Ltd. for the loan of the alloys, and in particular Mr. B. TAYLOR for the production and analysis of these.

REFERENCES

1 J. C. WOOLLEY AND B. BATES, *J. Less-Common Metals*, 1 (1959) 382.
2 M. HANSEN, *Constitution of Binary Alloys*, McGraw-Hill Book Co., New York, 1958.
3 U. ESCH AND A. SCHNEIDER, *Z. Electrochem.*, 50 (1944) 268.
4 A. I. APTEKAR AND B. N. FINKELSTEIN, *J. Exptl. Theoret. Phys. (U.S.S.R.)*, 21 (1951) 900.
5 H. K. HARDY AND T. J. HEAL, *Inst. Metals Monograph and Rept. Series*, No. 18 (1955) 1.
6 J. B. NEWKIRK, R. SMOLUCHOWSKI, A. H. GEISLER AND D. L. MARTIN, *J. Appl. Phys.*, 22 (1951) 290.

THE EQUILIBRIUM DIAGRAM OF THE SYSTEM MOLYBDENUM–RHODIUM

E. ANDERSON AND W. HUME-ROTHERY

The Dept. of Metallurgy, The University Museum, Oxford (Great Britain)

(Received February 10th, 1960)

SUMMARY

The equilibrium diagram of the system Mo–Rh above 1500°C, in the composition range 40–100 at. % Rh, has been investigated by a combination of thermal, microscopical and X-ray methods. The system contains an intermediate c.p. hexagonal or ε-phase extending from roughly 45–82 at. % Rh, the freezing point of which rises to a maximum at about 67 at. % Rh. Rh can dissolve about 15 at. % Mo at high temperatures. The lattice spacing/composition relations of the ε-phase are such that both a and c spacings diminish with increasing Rh content, but the axial ratio c/a passes through a minimum in the region of 75 at. % Rh. A similar characteristic is shown by the ε-phase of the system W–Ir, but not by the corresponding phases in the systems Mo–Ir or W–Rh. Other lattice-spacing relations are discussed, and the hardness of the alloys was also determined.

INTRODUCTION

The constitution of Mo-rich Mo–Rh alloys has been investigated by HAWORTH AND HUME-ROTHERY[1], who showed that, apart from the solid solution of Rh in Mo, a c.p. hexagonal or ε-phase exists in the equiatomic region. RAUB[2] studied this system below 1400°C, and showed that at 1300°C the composition limits of the ε-phase were approximately 50–85 at. % Rh, whilst the solid solution of Mo in Rh was determined as lying between 93–100 at. % Rh. The present paper describes an investigation of the system at higher Rh contents than those of HAWORTH AND HUME-ROTHERY, and the complete diagram (Fig. 1) is now known above 1500°C.

EXPERIMENTAL

The alloys used in the present work were kindly prepared by Murex Limited, and the authors must express their thanks to Dr. G. L. MILLER for his care and attention.

The specimens were prepared in the form of small bars from pure Mo powder (0.01% , 0.005% Fe, 0.03% lime, alkali metals and silica, and 0.05% O), and from pure h powder obtained from Messrs. Johnson, Matthey & Co., Limited; this contained 0.04% of non-metallic impurities (chiefly oxygen), and $<$ 0.05% of metallic mpurities, mainly Pt-group metals and Fe, Ag and Cu. The thoroughly mixed powers were cold-pressed at 30 tons/in.^{2}, and then sintered in hydrogen for 90 min t temperatures varying from 1680°–1760°C according to the exact composition. his treatment greatly reduced the oxygen content, and the resulting alloys in the

ε-field had a fine-grained structure (Fig. 2). Alloys consisting of the Rh-rich solid solution showed slightly larger grains (Fig. 3).

The method of quenching described by HAWORTH AND HUME-ROTHERY[1] for the

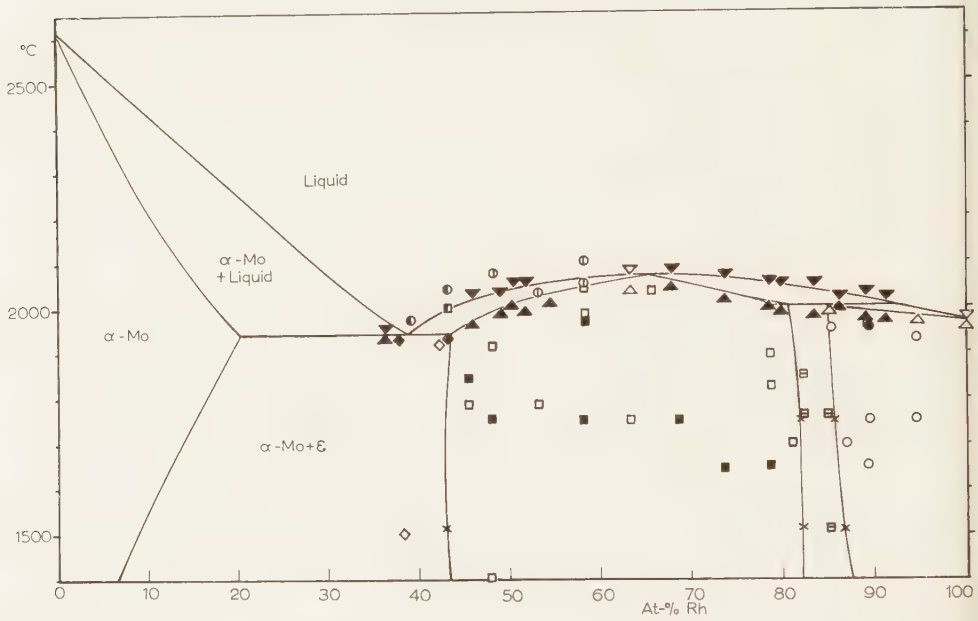

Fig. 1. Mo–Rh equilibrium diagram: ⧗, thermal arrests; ○, α-Rh; □, ε; ⊟, ε + α-Rh; ⦶, quenched liquid; ⊡, ε + liquid; ◇, ε + α-Mo; ×, X-ray points.

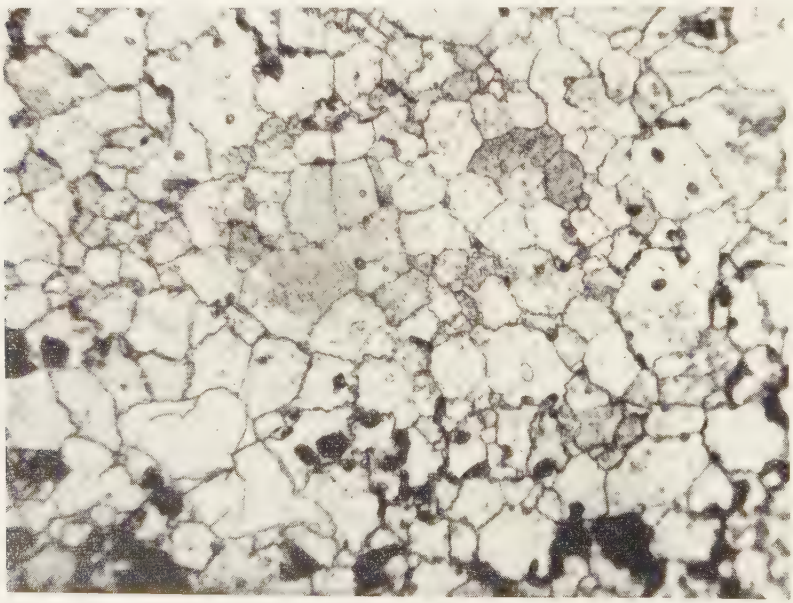

Fig. 2. Alloy Mo–48.6 at. % Rh (× 300). As sintered

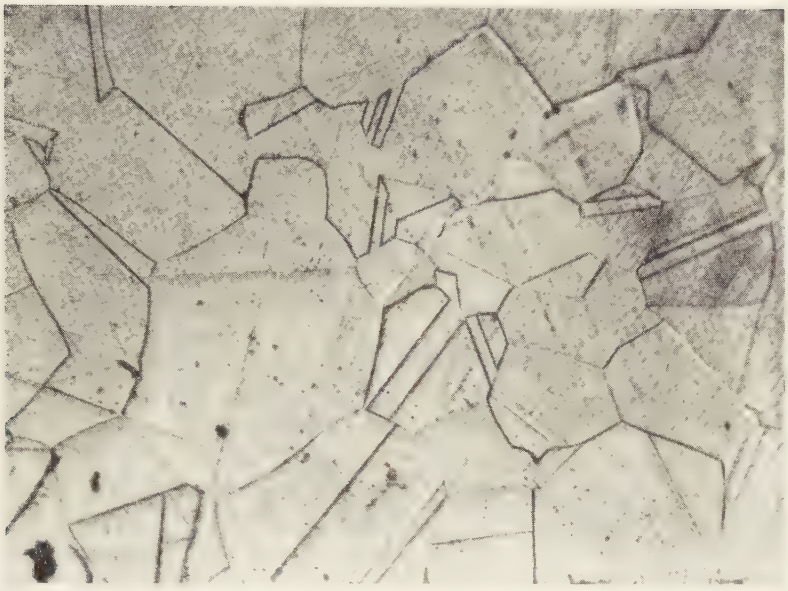

Fig. 3. Alloy Mo–89.4 at. % Rh (× 300). As sintered.

termination of the liquidus curve of Mo-rich alloys was not suitable for the Rh-h alloys of narrow freezing range. The liquidus curve was, therefore, determined by rmal analysis in an atmosphere of pure argon. Optical pyrometry was used for measurement of the temperature of a small specimen heated in a zirconia crucible ntained in an enclosure in which black-body conditions were obtained. For this rpose a special furnace, denoted Mark III, was designed and is described in the

g. 4. Thermal analysis result for pure Rh. Heating and cooling curves.

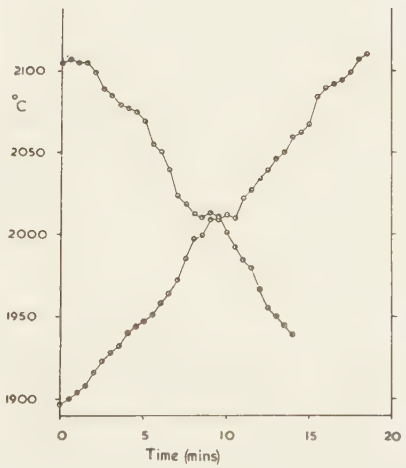

Fig. 5. Thermal analysis result for alloy Mo–86.2 at. % Rh. Heating and cooling curves.

Appendix. Temperature measurements were made by means of a Tinsley double range disappearing filament optical pyrometer which was calibrated against a W strip lamp standardised at the National Physical Laboratory*. The scatter of points when measuring a source at constant temperature is of the order ± 5°C and this prevents thermal arrests being read to a very high degree of accuracy. Fig. 4 shows heating and cooling curves for a specimen of pure Rh, and Fig. 5 shows corresponding curves for alloy 86.2**.

The solidus curves were first determined approximately by the microscopical examination of specimens quenched from successive temperatures, and then more accurately from arrests on heating curves taken in an atmosphere of purified argon.

Metallographic surfaces of the Rh-rich alloys were prepared by polishing with 2 μ grade diamond paste on a selvyt cloth and etching in a solution of 200 ml 20% HCl + 1–2 ml H_2O_2 with an alternating current of 0.1 A/cm^2 for the α-Rh solid solution alloys, and 0.3 A/cm^2 for ε-phase specimens. The etching times varied between 30 sec for α-Rh and 5 min for the ε-phase.

The solid solubility curves at high temperatures were determined by microscopical examination of specimens quenched after annealing in purified argon for periods varying from 10 min to 2 h. Additional points were also obtained by measuring the lattice spacings of the phases present in 2-phase (α Mo + ε) and (ε + Rh) alloys. For this purpose, lumps of the 2-phase alloys were first annealed for 1–2 hours at the temperatures concerned, and were then quenched and ground to powder in a WC mortar. The filings were then heated to the same temperature and quenched, and the lattice-spacings determined by standard methods using a 19 cm Unicam camera, and CuKα radiation. All high-temperature annealing work was carried out in the Mark I and Mark II W resistor furnaces of HAWORTH AND HUME-ROTHERY[1].

THE EQUILIBRIUM DIAGRAM

The results of the present work are shown in Fig. 1 in which the full points refer to specimens analysed after the experiments concerned. For the open points, the compositions are either taken to be the same as the analytical values for another specimen of the same bar, or are the synthetic values.

The liquidus curve for the ε-phase rises to a maximum (2075 $\pm$ 10°C) at a composition corresponding to approximately 2 atoms of Rh: 1 atom of Mo. The curve then sinks to a peritectic horizontal at 2000 $\pm$ 10°C corresponding to the reaction: Liquid (92 at. % Rh) + ε (81 at. % Rh) $\rightleftarrows$ Solid solution in Rh (85 at. % Rh).

The freezing ranges for both the ε- and Rh-rich solid solutions are very small, in marked contrast to those for the Mo-rich solid solution.

LATTICE SPACING RELATIONS

Table I and Fig. 6 show the lattice spacing/composition relations for the ε-phase. All points refer to analysed alloys and, as the powder films were of good quality, the lattice spacings should be accurate to within $\pm$ 0.0002 kX.

In the ε-phase, both a- and c- spacings contract with increasing Rh content, but the curve for the c-spacing shows a change in direction at about 74 at. % Rh, and this

* See HAWORTH AND HUME-ROTHERY[1].

** For abbreviation, alloys are referred to by their atomic percentages of Rh.

TABLE I

(a) LATTICE PARAMETERS OF THE ε-PHASE IN THE SYSTEM Mo–Rh

Rh (at. %)	*Annealing temp. (°C)*	*Time (h)*	*Ao, kX*	*Co, kX*	*c/a*
38.3 (2-phase)	1505	2	2.7617	4.4499	1.6113
45.2	1700	1	2.7541	4.4258	1.6070
48.1	1700	1	2.7502	4.4119	1.6042
55.5	1680	1	2.7426	4.3895	1.6005
58.7	1750	1	2.7400	4.3818	1.5992
69.2	1700	1	2.7278	4.3549	1.5965
73.9	1650	1	2.7226	4.3412	1.5945
78.8	1670	1	2.7185	4.3387	1.5960
80.9	1760	1	2.7144	4.3376	1.5980
85.1 (2-phase)	1750	1	2.7146	4.3415	1.5993
85.1 (2-phase)	1510	2	2.7144	4.3414	1.5994

(b) LATTICE PARAMETER OF THE α-Rh SOLID SOLUTION ALLOYS IN THE SYSTEM Mo–Rh

Rh (at. %)	*Annealing temp. °C*	*Time (h)*	*Ao, kX*
Pure Rh	—	—	3.7954
94.7	1800	1	3.8010
91.5	1810	1	3.8046
89.4	1800	1	3.8066
85.1 (2-phase)	1750	1	3.8108
85.1 (2-phase)	1510	2	3.8100

roduces a marked increase in the axial ratio. As the change occurs so near to the 1 atomic ratio, it is probable that it is related to the formation of a superlattice ther than to an electronic (Brillouin zone) effect. The atomic numbers of Mo and h are, however, too close together for superlattice lines to be detected easily.

The lattice spacing/composition relations for the solid solution in Rh are shown

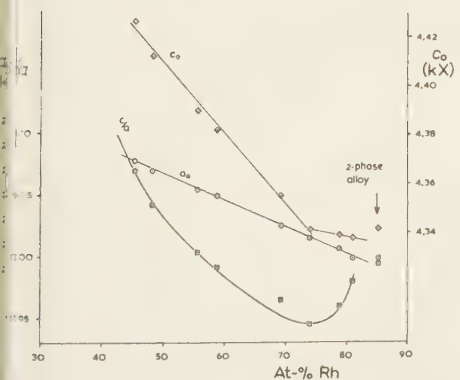

Fig. 6. Lattice spacing/composition relations for the ε-phase in the Mo–Rh system.

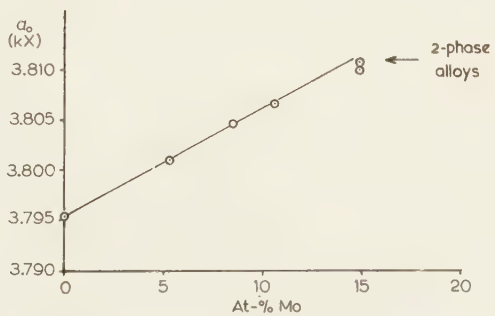

Fig. 7. Lattice parameter results for the Rh-rich solid solution in the Mo–Rh system.

in Table I and Fig. 7. The lattice spacing of Rh is expanded by solution of Mo, and the significance of these results is discussed below.

HARDNESS TESTS

Fig. 8 shows the V.P. Hardness figures for the sintered alloys (annealed at 1750° ± 20°C) containing 45–100 at. % Rh. For pure Rh the measured value of 116 may be compared with 100 V given by VINES[3].

The hardness of Rh is increased by the solution of Mo, and in the ε-phase region the increase continues at a slower rate, but the 2-phase alloys show anomalous results.

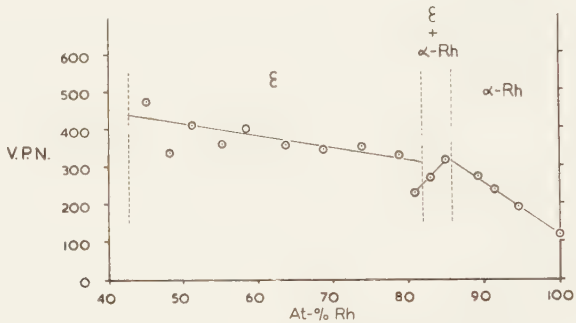

Fig. 8. Vickers Pyramid Hardness data for Mo–Rh alloys.

DISCUSSION

Close-packed hexagonal phases

The composition-range of the close-packed hexagonal Mo–Rh ε-phase agrees with the principle advanced by HAWORTH AND HUME-ROTHERY[4], and there is a general movement in the direction of higher Mo-content on passing from Mo–Ru → Mo–Rh → Mo–Pd.

In the system Cr–Co there is no intermediate phase corresponding to the ε Mo–Rh phase*, but in the system W–Ir[5] there is an analogous c.p. hexagonal phase and,

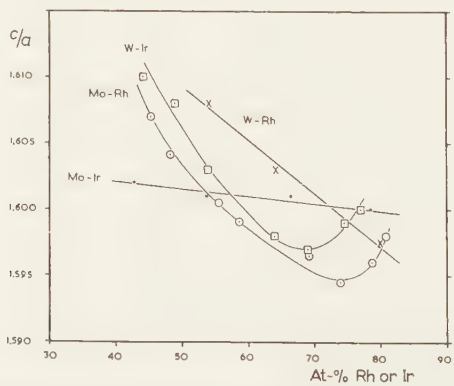

Fig. 9. Axial ratio/composition relations of the ε-phases in the following systems: ⊙, Mo–Rh; •, Mo–Ir; ×, W–Rh; ⊡, W–Ir.

* The extreme limit of the solid solution of Cr in c.p. hexagonal Co overlaps the composition range of the ε Mo–Rh phase, but lattice spacing data are not available for the Co alloys.

s shown in Fig. 9, the axial ratio of this passes through a minimum in the region of
·o at. % Ir. This behaviour is not shown by the corresponding Mo–Ir c.p. hexagonal
hase[2], and probably not by the W–Rh ε-phase[5], although only three alloys have
iere been investigated. It seems, therefore, that the formation of the minimum is
onfined to systems in which the two metals are in the same row of the Periodic
Table.

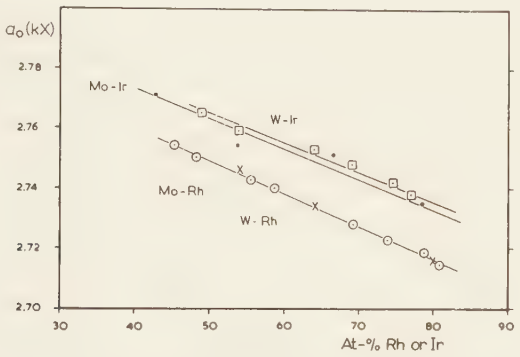

Fig. 10. *a* spacing/composition relations of the ε-phases in the following systems: ○, Mo–Rh; ●, Mo–Ir; ×, W–Rh; ⊡, W–Ir.

The ε-phases are remarkable for the fact that, as shown in Fig. 10, the *a* spacings
f the Mo Rh and W–Rh ε-phases are identical functions of the composition, and
he *a* spacings of the Mo–Ir and W–Ir phases are also similar, although the experi-
ental accuracy is here less. The *c*-spacings are, however, not the same in the different
stems. If the straight lines in Fig. 10 are extrapolated to 100% Rh and Ir, they
ead to *a* values of 2.694 kX and 2.714 kX respectively, as compared with closest
istances of approach in the face-centred cubic structures of 2.684 (Rh) and 2.709
Ir). There is general agreement that in the elements of Group VIIIB the electron
louds of the outer *d* electrons are becoming repulsive or atomic in nature, whilst in
he Group VI elements all the outer electrons are concerned in the cohesion, and the
tomic cores are small. It seems possible, therefore, that in these ε-phases the *a*
pacings are determined by the element of Group VIIIB modified by an electronic
ffect involving the difference between the Group numbers VIA and VIIIB, whilst
he *c* spacings are much more sensitive to the minor differences between the different
lements.

Atomic volume relations

The Mo Rh equilibrium diagram involves phases with the three typical metallic
tructures. According to GOLDSCHMIDT[6] there is a contraction of 3% in the atomic
liameter in passing from co-ordination number [12] → [8]. This contraction is such
hat the atomic volume remains almost exactly constant. It appears that this fact
as not been pointed out in the published literature, although correspondence with
Professor MOTT shows that it has been realised for some time at both Oxford and
Cambridge, and Professor MOTT considers that the relationship follows naturally
rom the current theory of metallic cohesion, at any rate for metals where *d*-orbitals

play only a small role. Fig. 11 shows the mean atomic volumes of the Mo Rh alloys as a function of the composition. In these alloys the *d*-fraction of the hybrid *spd* orbitals is considerable, but the deviations from an "atomic volume Vegard's Law" are comparatively slight. The points for the ε-phase lie on a straight line which, on

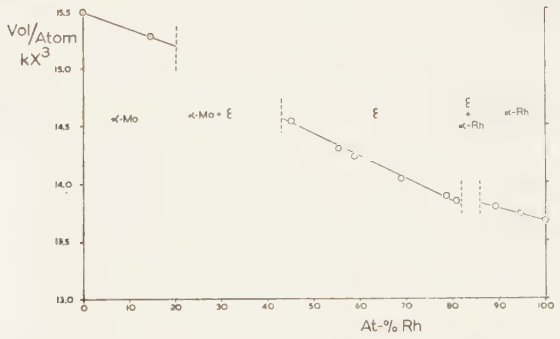

Fig. 11. Atomic volume/composition relations in the Mo–Rh system.

extrapolation, passes almost exactly* through the point for pure Mo, but slightly below that for pure Rh. The solid solutions in Mo and Rh show positive and negative deviations respectively from an atomic volume Vegard's Law. This may be due to the fact that, as explained above, the atomic core of Mo is relatively small, so that the substitution of Rh for Mo involves the introduction of a larger core, which is not involved by the substitution of Mo for Rh.

APPENDIX

A High Temperature Furnace for Thermal Analysis in the Range 1500–2200°C

Haworth and Hume-Rothery[1] described two tube resistor furnaces (Marks I and II) in which the heating elements consisted of cylinders of W foil, the ends of which fitted into water-cooled Cu blocks, the whole being maintained in a vacuum or inert atmosphere. Although excellent for annealing work, these furnaces were unsuitable for thermal analysis because they gave unsteady rates of heating and cooling. This was probably due to poor contact between the W cylinder and the Cu blocks, and a completely new furnace has therefore been designed (Mark III) (Fig. 12).

In the Mark III furnace, the heating element is of Ta shaped as shown in Fig. 13. The end of the heating element is fitted into water-cooled Cu blocks by means of the device shown in Fig. 14. The Ta sheet is held between the Cu blocks and two curved pieces of 1/16 in. Mo strip. The latter are tapped so as to take 4BA Allen screws, by means of which the Ta sheet is pressed tightly against the Cu, and in this way a good contact is assured.

The Ta heater is surrounded by a set of twelve cylindrical Mo radiation screens H with an innermost screen of W as shown in Fig. 12. The water-cooled copper electrodes D are insulated from the base-plate X by sealing O-rings and Tufnol washers, and are connected by heavy Cu strip to the secondary of a 16:1 step-down transformer, whose primary is supplied by a type 50B Variac transformer. When running at 2000°C, the power consumption is 200 A at 12 V.

* A straight line could be drawn from the value for pure Mo.

The specimen is contained in a small thoria or zirconia crucible G (21 mm × 13 mm diameter) resting on the stand tube F of hollow Mo rod, which stands on the alumina tube E. The electrode assembly of Fig. 12 is surrounded by a water-cooled brass cover whose top contains a hole, covered by a glass prism through which the specimen can be viewed with an optical pyrometer.

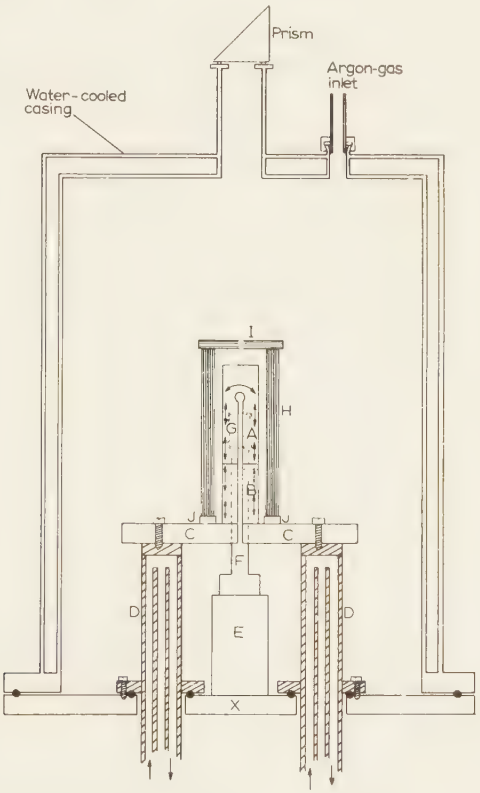

Fig. 12. Mark III furnace: A, upper part of heater, of 0.004 in. Ta sheet; B, lower part of heater made of thicker sheet than (A); C, Cu blocks; D, water-cooled Cu electrodes; E, alumina stand-tube; F, Mo stand-tube; G, zirconia or thoria crucible and lid; H, cylindrical set of radiation screens; I, upper set of radiation screens; J, small alumina studs; X, brass base-plate.

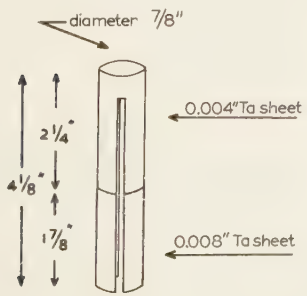

Fig. 13. Mark III heating element.

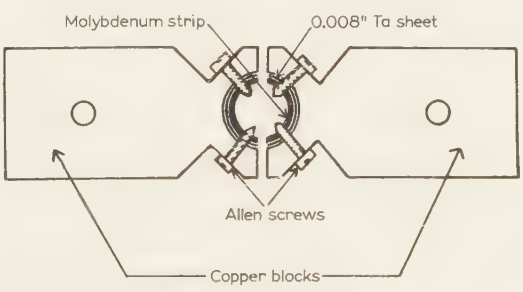

Fig. 14. Plan of Mark III electrode assembly.

The top of the crucible is covered by a lid bored with a 1.5 mm diameter hole through which the specimen (7 - 10 g) is viewed. Black-body conditions are obtained by arranging that the ratio of the height of the empty space in the crucible above the specimen to the diameter of the hole in the lid is at least 6:1.

Temperatures were measured by means of a Tinsley double range, disappearing filament optical pyrometer, and the accuracy of the apparatus tested by determining the melting points of Pd, Pt and Rh with the results shown in the tables given below. There is a general tendency for cooling curve arrests to be slightly higher than the heating curve arrests but the effect is not serious and the measured values of the melting points agree with the accepted values to within the limits of the experimental accuracy which is of the order $\pm$ 10°C. It is, however, necessary to take great care that the crucible is situated in the region of most constant temperature in the furnace. If this precaution is not taken, the difference between values obtained on heating and cooling may be as much as 40°C.

MELTING POINT (°C) DETERMINATIONS ON PURE METALS

Palladium	*Heating curve*	*Cooling curve*	*Mean value*
Melting point	1550	1556	1553
	Accepted melting point*:	1552	
Platinum	*Heating curve*	*Cooling curve*	*Mean value*
Melting point	1758	1765	1762
		1766	
	Average value for melting point: 1764		
	Accepted melting point*: 1769		
Rhodium	*Heating curve*	*Cooling curve*	*Mean value*
Melting point	1966	1962	1964
	1959	1972	1966
	1960	1968	1964
	1957	1965	1961
	1963	1973	1968
Averages	1961	1968	1965
	Accepted melting point*:	1966	

* *Metals Reference Book*, C. J. SMITHELLS

REFERENCES

[1] C. W. HAWORTH AND W. HUME-ROTHERY, *J. Inst. Metals*, 87 (1958–59) 265.
[2] E. RAUB, *Z. Metallk.*, 45 (1954) 23.
[3] R. F. VINES, *The Platinum Metals and Their Alloys*, International Nickel Co., New York, 1941.
[4] C. W. HAWORTH AND W. HUME-ROTHERY, *Phil. Mag.*, 3 (1958) 1013.
[5] E. RAUB AND P. WALTER, *Festschrift aus Anlass des 100-jährigen Jubiläums der Firma W. C. Heraeus G.m.b.H.*, Hanau, 1951, p. 124.
[6] V. M. GOLDSCHMIDT, *Z. physik. Chem.*, 133 (1928) 397.

THE PREPARATION OF HIGH PURITY VANADIUM PENTOXIDE BY A CHLORINATION PROCEDURE*

ROBERT E. McCARLEY AND JAMES W. RODDY

Institute for Atomic Research and Dept. of Chemistry, Iowa State University, Ames, Iowa (U.S.A.)

(Received March 7th, 1960)

SUMMARY

A method for the preparation of high purity V_2O_5 from a technical grade oxide has been developed. The method includes the reaction of the impure oxide with Cl and C, hydrolysis of the resultant $VOCl_3$ in aqueous NH_3, and ignition of the precipitated NH_4VO_3 at 500–600°C. V_2O_5 containing a maximum of *ca.* 100 p.p.m. impurities was produced in kilogram quantities both cheaply and efficiently by this process.

INTRODUCTION

Large quantities of a low grade oxide, which corresponds roughly to the composition $Na_4H_2V_{10}O_{28}$ and which is commonly called "red cake", are available as a by-product of the processing of U ores. Because of the need in this laboratory for high purity V oxides in the preparation of V metal, a method was sought for the production of V_2O_5 of exceptional purity. The method described here utilized the readily available "red cake" as the starting material and yielded a product having the degree of purity desired.

The decision to investigate a chlorination procedure was prompted by the relatively low cost of the necessary reagents and the advantages which a volatile liquid intermediate, *e.g.* $VOCl_3$, offered for purposes of purification. High purity reagent grade V_2O_5 has been prepared[1] from solutions of commercial V_2O_5 in aqueous Na_2CO_3 by precipitation of NH_4VO_3 with NH_4Cl. Removal of Fe, Si and Al impurities depended upon precipitation by correct adjustment of pH and filtration prior to the formation of NH_4VO_3. This procedure is less than satisfactory where V_2O_5 of very high purity is desired.

EXPERIMENTAL

Chlorination procedure

The V "red cake" used in this investigation was obtained from Lucius Pitkin, Inc. in dense, flake form; it contained *ca.* 88% V_2O_5 by weight. Spectrographic analysis indicated the presence of considerable quantities of Mg, Na, Al, Ca, Cu, Si and Mn

This work was performed in the Ames Laboratory of the U.S. Atomic Energy Commission and Contribution No. 835.

along with lesser quantities of Fe, Cr, Mo, Nb and Ti. Subsequent to use, this material was ground to a fine powder in a hammer mill.

The reaction charge consisted of an intimate mixture of 1100 g of the "red cake" and 100 g of carbon black. Based on the actual content of V_2O_5 in the red cake this mixture corresponded to a 3 : 2 mole ratio of C : V_2O_5. This ratio of reactants was used since preliminary reactions using c.p. V_2O_5 indicated that the stoichiometry of the reaction was described by the equation

$$2\ V_2O_5 + 3\ C + 6\ Cl_2 = 4\ VOCl_3 + 3\ CO_2$$

Prior to chlorination, the mixture was dried in the reaction tube by passing air over the solids at 400° C.

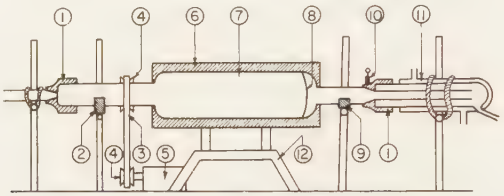

Fig. 1. Chlorination apparatus: 1. saran rubber cap; 2. four inch casters; 3. belt; 4. pulley; 5. variable speed motor; 6. split-winding furnace; 7. reaction tube, 100 mm × 450 mm; 8. perforated glass plate with holes approximately 3 mm in diameter; 9. two-inch casters; 10. syringe; 11. precondenser and iron chloride trap; 12. furnace support.

After complete removal of moisture, the apparatus for the chlorination reaction was assembled as shown in Fig. 1. On each end of the reaction tube was placed a saran rubber cap machined so that a tight rotating seal resulted when it was connected to a 24/40 glass joint. A neoprene rubber gasket, which was protected from the reaction vapors by a teflon washer, provided a vapor-tight seal between the reaction tube and the saran cap. Silicone grease was used as the lubricant for these rotating seals. At the exit end of the reaction tube a small syringe filled with the grease was inserted through

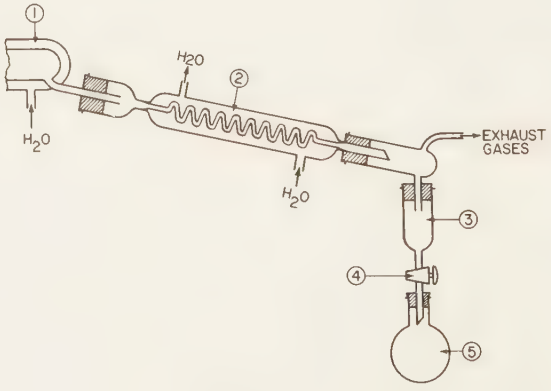

Fig. 2. Condensing system for $VOCl_3$: 1, precondenser and iron chloride trap; 2, Graham condenser; 3, measuring separatory funnel; 4, teflon stopcock; 5, receiving flask.

ne saran cap. This provision made it possible to renew the supply of lubricant while ne reaction was in progress.

When the desired furnace temperature had been attained, rotation of the reaction ibe was begun and Cl gas at a measured flow rate was admitted. The product $VOCl_3$ as liquefied in a water condenser and collected in a large receiving flask while other aseous products were conducted to the hood through a sulfuric acid scrubber. In nose cases where the percent conversion of Cl was to be measured, the collection ssembly illustrated in Fig. 2 was used. Thus it was possible to obtain the percent ilorine conversion as a function of time, temperature and flow rate by measuring olumetrically the rate of production of liquid $VOCl_3$.

istillation and hydrolysis of $VOCl_3$

Distillations of the $VOCl_3$ were performed in a 25 mm O.D. pyrex column which was ked with glass helices to a height of 18 in. The column and receiving vessel were otected from the atmosphere by a drying tube containing anhydrous $CaCl_2$.

In the early stages of this investigation the $VOCl_3$ was hydrolyzed by dropwise ldition of the liquid to reagent grade NH_4OH with rapid stirring. However, this ocedure was found to be unsatisfactory for two reasons. Owing to the violence of the drolytic reaction considerable loss of V occurred by volatilization and significant uantities of Si were introduced into the product from the reagent grade NH_4OH. ese difficulties were overcome by preparation of the NH_3 solutions from gaseous, hydrous NH_3 and by introducing the $VOCl_3$ below the surface of the solution at a ntrolled rate. For this procedure a 5 gal. pyrex vessel containing 15 l of 3 *M* NH_3 lution was used. Approximately 1 l of $VOCl_3$ was added at a dropwise rate from ur 250 ml separatory funnels equipped with teflon plugs. Gaseous NH_3 was intro-ced continuously during the course of the hydrolysis to maintain the concentration *ca.* 3 *M*, and the mixture was stirred rapidly with a large propeller-type glass stirrer. llowing the completion of the hydrolysis it was necessary to allow the precipitate NH_4VO_3 to stand in contact with the mother liquor for at least 6 h to insure com-ete precipitation of the vanadium. The solids were then separated by filtration on rge fritted glass buchner funnels and air dried at *ca.* 200° C.

Ignition of the NH_4VO_3 was carried out in a rotating vycor tube similar to that own in Fig. 1. Best results were obtained when air was passed continuously over the lids at temperatures from 500 to 600° C. The V_2O_5 produced in this way was a free-owing powder which possessed a bright orange color.

nalytical

All V analyses were performed in the usual manner, *i.e.* by titration with standard rmanganate solution after prior reduction of the V with SO_2. The concentration of purities in the V_2O_5 was determined spectrographically*. Only those elements hich were found to be present by a preliminary spectrographic survey were deter-ined quantitatively. N was determined volumetrically as NH_3 after distillation from ne basic solution formed by dissolving V_2O_5 in aqueous NaOH.

All spectrographic analyses were performed by the spectroanalytical group of this laboratory.

Precipitation and masking agent studies

In order to determine the optimum NH_4 ion concentration needed to effect precipitation of the NH_4VO_3, solutions containing known amounts of V were prepared by fusion of c.p. V_2O_5 with NaOH and dissolving the Na vanadate in water. Aliquots of these solutions were then added to solutions of NH_4Cl at various concentrations to precipitate the NH_4VO_3. The percent of V precipitated was determined by filtration of the NH_4VO_3 on tared, sintered glass crucibles, followed by ignition at 500° C and weighing as V_2O_5.

The results of these experiments indicated that for concentrations of vanadate of 0.18 – 1.5 *M* in the aqueous solutions, a final concentration of NH_4^+ of 2.5–3.0 *M* was needed to precipitate 99% of the V. In the presence of 3.0 *M* NH_4Cl the efficiency of the removal of V from the solutions was decreased only very slightly by the addition of up to 3000 p.p.m. of citrate, tartrate or ethylenediaminetetraacetic acid. Consequently, 3.0 *M* NH_4OH was chosen as the hydrolysis medium for the $VOCl_3$, since NH_4Cl was produced as the hydrolysis proceeded according to the equation:

$$VOCl_3 + 4\ NH_4OH = NH_4VO_3 + 3\ NH_4^+ + 3\ Cl^- + 2\ H_2O$$

The volumes of $VOCl_3$ and the hydrolysis solution were chosen so that the final concentration of NH_4Cl was about 2.5–3.0 *M*.

RESULTS AND DISCUSSION

Chlorination

Table I shows the efficiency of Cl utilization at various flow rates and at the furnace temperatures of 350 and 450° C. Each value of the percent conversion represents the average of three separate determinations whose average deviation was not more than ± 2 percentage units. At the lower temperature, a maximum Cl efficiency of 84% was realized at a flow rate of 2.70 l/min. However, the actual charge temperature reached a maximum at this same point and doubtless was responsible for the higher efficiency because of increased reaction rate. On the other hand, at still higher flow rates the efficiency decreased as a result of cooling of the reaction charge owing to the more rapid transport of gases through the system. At the furnace temperature of

TABLE I

VARIATION OF PERCENT Cl CONVERSION AND CHARGE TEMPERATURE WITH Cl FLOW RATE

Furnace temp. 350°C			*Furnace temp. 450°C*		
Cl flow rate (l/min)	*Percent Cl conversion*	*Charge temp. (°C)*	*Cl flow rate (l/min)*	*Percent Cl conversion*	*Charge temp. (°C)*
0.69	56	365	1.00	91	465
1.00	57	373	1.46	96	468
1.69	68	380	1.72	96	470
1.80	67	389	1.90	92	470
2.20	70	402	2.16	94	470
2.42	82	418	2.52	92	468
2.60	83	424	3.00	97	468
2.70	84	430	3.48	93	470
3.00	79	413	4.20	96	467
4.32	78	407			

350° C the rate of chlorination is seen to be sufficiently rapid so that the Cl efficiency is very high and practically independent of the flow rate up to 4.2 l/min.

The total Cl efficiency for the complete conversion of the available V is somewhat lower than the data in Table I would indicate. This observation is demonstrated by the data in Table II, which also shows that, regardless of the operating temperature, a maximum of only 76% V was extracted from the "red cake" by this procedure. The variation of Cl efficiency at progressive intervals during the course of the reaction is

TABLE II

TOTAL Cl EFFICIENCY AND PERCENT V CONVERSION

Furnace temp. (°C)	*Cl flow rate (l/min)*	*Percent Cl conversion*	*Percent V conversion*
350	2.00	58	75
350	2.45	62	76
350	2.60	65	75
450	1.90	90	76
450	2.00	89	75

given in Table III for the two furnace temperatures and a Cl flow rate of 2.0 l/min. At either temperature the efficiency decreased near the end of the reaction, as expected, but at 450° the decrease was much more rapid. Consequently, the total Cl efficiency for the process remained close to 90% at the higher temperature. Continuation of the reaction beyond the point described by the data resulted in little additional conversion of the V.

TABLE III

VARIATION OF Cl EFFICIENCY AS THE REACTION PROGRESSED AT CONSTANT FLOW RATE

$VOCl_3$[a] produced (ml)	*Percent Cl[b] conversion*	*Percent Cl[c] conversion*
300	85	96
350	85	96
400	86	97
450	90	96
500	85	93
550	85	91
600	67	88
650	50	85
700	34	65
750	12	10

[a] Volume produced prior to determination of the Cl efficiency.
[b] Determined at a furnace temperature of 350°C.
[c] Determined at a furnace temperature of 450°C.

The residues, after the termination of the reactions, had agglomerated into small balls which appeared to have been formed by fusion of the material. In experiments with a static bed of the carbon-red cake mixture, a similar effect was noticed. In this case a crust, which effectively prevented further chlorination, was formed at the surface of the mixture at a much earlier stage of the reaction. It must be assumed then that this crust was relatively non-porous, and once formed, acted as a protective coating on the particles so that chlorination effectively ceased.

Distillation and hydrolysis

An evaluation of the removal of certain impurities from the $VOCl_3$ by distillation was obtained by fractionation of the crude material obtained from the chlorination reaction. Samples of the distillate were taken at regular intervals during the course of the distillation and treated as previously described for conversion to V_2O_5. The samples of V_2O_5 were then analyzed for their impurity content. Results of this experiment are given in Table IV. Although complete removal of the elements present as the

TABLE IV

THE EFFECT OF DISTILLATION OF $VOCl_3$ ON THE V_2O_5

Sample No.	Spectrographic analysis (p.p.m.)						
	Si	*Fe*[a]	*Mg*[a]	*Cr*[a]	*Cu*	*Ti*	*Ca*[a]
1[b]	105	<100	<20	<20	50	40	30
2	150				30	~13	<20
3	50				27	~16	<20
4	35				25	20	<20
5	35				22	22	<20
6	30				25	23	<20
7	33				20	25	<20
8	35				22	20	<20
9	34				24	~17	<20
10	33				25	20	<20
11	35				23	~16	<20
12	35				20	~14	<20
13[c]	75	↓	↓	↓	50	43	35

[a] Limit of standard curve for determination of Mg, Cr and Ca was 20 p.p.m.; for Fe, 100 p.p.m.
[b] Analysis of sample before distillation.
[c] Analysis of pot residue after distillation.

principal impurities was not accomplished by distillation, a considerable reduction in their concentration was attained. The rather constant concentrations of Si, Cu and Ti found in samples 4–12 indicated that with the fractionating column used, further purification from these elements was not possible. It did not seem feasible to construct a more efficient column since it was found that these elements were readily removed by addition of either citric or tartaric acid during the hydrolysis step. Furthermore, the distillation step need not be included at all with the use of the masking agents, unless the ultimate in purity is desired.

In Table V are given the quantitative spectrographic analyses of several samples of V_2O_5 prepared by hydrolysis of the $VOCl_3$ in the presence of the complexing agents, citric and tartaric acids. Thus, addition of these reagents to the hydrolysis solution was shown to remove all impurity elements retained in the $VOCl_3$, with the exception of Si, to the limits of the method of their determination. Elements not listed in Tables IV and V were not detected. Analysis of the product V_2O_5 for V gave results in the range 55.90–56.00% V; calculated value for V_2O_5 was 56.02%. These results indicate the product to have the exact composition V_2O_5 within the experimental error of the method employed. Estimation of the purity of the V_2O_5 by summation of the impurity concentrations leads to a value of *ca.* 99.99%.

Ignition of ammonium metavanadate

In the initial experiments, the precipitates of NH_4VO_3 were placed in silica boats

TABLE V

THE EFFECT OF COMPLEXING AGENTS ON PURITY OF V_2O_5

Sample No.	*Complexing agent*	*Conc. of complexing agent (p.p.m.)*	*Spectrographic analysis (p.p.m.)*					
			Si[a]	*Mg*[a]	*Cr*[a]	*Ti*[a]	*Ca*[a]	*Fe*
1[b]	citric acid	1000	25	<20	<20	<20	<20	~30[d]
2	citric acid	1000	<20	↓	↓	↓	↓	~30[d]
3	citric acid	1000	22	↓	↓	↓	↓	ND[e]
4	citric acid	1000	<20	↓	↓	↓	↓	ND
5	citric acid	1000	<20	↓	↓	↓	↓	ND
6	citric acid	1000	<20	↓	↓	↓	↓	ND
7[c]	citric acid	1000	<20	↓	↓	↓	↓	~30[d]
8	citric acid	600	<20	↓	↓	↓	↓	ND
9	tartaric acid	1000	<20	↓	↓	↓	↓	ND
10	none added	—	24	↓	↓	↓	↓	ND

[a] Limit of the spectrographic method of determination for these elements was 20 p.p.m.
[b] Sample of V_2O_5 obtained from $VOCl_3$ which had not been distilled.
[c] Sample of V_2O_5 obtained from $VOCl_3$ which was left as pot residue after distillation.
[d] When determined by a colorimetric method, only 11 p.p.m. Fe was found.
[e] Not determined.

[a]l calcined under static conditions in a muffle furnace. When this procedure was [l]owed with quantities of several hundred grams, several of the products were not [t]e normal orange color of V_2O_5, but were olive drab in appearance. An analysis for [i]n these samples gave V contents 1–2% lower than that calculated for V_2O_5. Even [t]hen these samples were heated to the fusion temperature in a current of air, a [n]oticeable improvement in their appearance or composition was not observed. This [d]ifficulty was effectively eliminated by ignition of the NH_4VO_3 in a rotating vycor [t]ube under a constant flow of air.

Since the reduction of the N content in the V_2O_5 to the lowest possible value was [d]esired, the effect of the ignition temperature was studied. The values of Table VI [i]ndicate that any temperature over 500° C is acceptable, but for very low N content, [t]emperatures over 600° C should be used. The ignition temperature had no noticeable [e]ffect upon the concentration of other impurities.

TABLE VI

EFFECT OF IGNITION TEMPERATURE UPON N CONTENT OF V_2O_5

Sample No.	*Ignition temperature*[a] *(°C)*	*Nitrogen content*[b] *(p.p.m.)*
1	500	32
2	525	13
3	540	16
4	575	22
5	600	12
6	625	0
7	650	5

[a] Time of ignition, 6 h.
[b] Limits of error, ±25%. Values <10 p.p.m., very approximate.

REFERENCE

[1] C. Tyzack and P. G. England, *Symposium on the Extractive Metallurgy of Some of the Less-Common Metals*, Inst. Mining Met., London (1956).

SOME OBSERVATIONS ON DECOMPOSITION OF METASTABLE BETA-PHASE IN TITANIUM–CHROMIUM ALLOYS

K. A. GROSS AND I. R. LAMBORN

Defence Standards Laboratories, Department of Supply, Maribyrnong (Australia)

(Received March 21st, 1960)

SUMMARY

A re-examination of the decomposition of metastable β-phase at 420°C and 500°C has shown no evidence in support of the formation of a supersaturated α-phase. It is suggested that the compound $TiCr_2$ is not precipitated directly from enriched β, but that the eutectoid decomposition results in precipitation of α and a transition phase γ'. $TiCr_2$ is subsequently formed from γ' on continued heating.

INTRODUCTION

A modification of the generally recognised sequence in decomposition of the metastable β-phase of eutectoid Ti alloys has been suggested by POLONIS AND PARR[1] for a Ti – 6% Ni alloy. This work indicated that decomposition involved precipitation of a supersaturated α-phase from which the γ-phase, Ti_2Ni, and α of equilibrium Ni content subsequently precipitated.

There is also some suggestion of the formation of a supersaturated α-phase in other Ti binary alloys[2,3]. That α-phase does appear to participate in the precipitation of $TiCr_2$ in Ti – Cr alloys has been indicated by the metallographic observations of FROST *et al.*[4] and ROSTOKER[5] in isothermally quenched Ti – Cr alloys at elevated temperatures. Whilst ROSTOKER suggests that the phenomenon results from the effects of interstitial impurities on the binary equilibrium diagram, the work of AARONSON *et al.*[6] indicates that it may be explained by alternate $TiCr_2$ and α-phase precipitation, with the $TiCr_2$ being engulfed by the α.

A further noteworthy feature of previous investigations of the Ti – Cr system is the divergence of opinion as to the criteria indicating the start of the eutectoid decomposition and the relative merits of metallographic and X-ray diffraction techniques for detection of $TiCr_2$.

Results of an investigation designed to examine further the β decomposition, particularly the eutectoid decomposition, in two hypoeutectoid Ti – Cr alloys are presented in the following sections.

MATERIAL AND EXPERIMENTAL PROCEDURE

The alloy used for the major part of the investigation contained 7.26 wt.% Cr and was made from high grade Ti sponge and electrolytic Cr. β-phase only could be detected in this alloy on water quenching from the β-field. After arc melting in purified argon the

i had a hardness of 110 on the diamond pyramid scale. The conditions of heating the β-field (*viz.* 790°C for 5 min) were selected to ensure a fine grain size to facilitate -ray examination. Specimens were one inch diameter discs cut from sheet.

Metallographic examination, hardness measurements, and bend tests were used in njunction with X-ray diffraction in a Philips Diffractometer with a flat specimen inner to follow β-decomposition at 420°C and 500°C. While most specimens were enched and reheated to these temperatures, some were isothermally quenched for mparison.

Needle specimens, produced by electropolishing and of large original β grain size re also used for X-ray studies at various stages of β decomposition. These were amined in a Unicam Goniometer, the patterns being recorded photographically.

An alloy containing 3.87 wt.% Cr, reheated at 500°C, was examined in a similar mer. Martensitic α-phase only could be detected in this alloy after quenching from β-field.

RESULTS

ce decomposition of the β-phase resulting from prior martensite decomposition in 3.87% Cr alloy at 500°C showed features similar to that of the retained β in the 26% Cr alloy, results for the latter alloy only will be reported in detail. Further, isothermally quenched specimens behaved similarly to the reheated specimens, main difference being more rapid transformation in the former at 500°C. Attention, refore, is confined to reheated specimens.

Except in the very early stages of decomposition at 500°C, metallographic examiion was unreliable for the detection of phase changes at both temperatures emyed. The phases present at various stages of decomposition, as indicated by X-ray ffraction, are shown in Tables I and II.

TABLE I

X-RAY DIFFRACTION DATA OBTAINED FROM Ti–7.26% Cr ALLOY AGED AT 420°C

Ageing time	*Phases present**	*% β_E Cr content (approx.)*	*% β_E (approx.)*
5 min	$\beta_o + \omega + \beta_E$	—	—
15 min	$\beta_o + \omega + \beta_E$	16	—
30 min	$\beta_o + \omega + \beta_E$	—	—
1 h	$\beta_o + \omega + \beta_E$	16	—
2 h	$\omega + \beta_o + \beta_E$	—	—
6 h	$\omega + \beta_E$	16	34
9 h	$\omega + \beta_E$	16	30
16 h	$\alpha + \beta_E$	26	32
24 h	$\alpha + \beta_E$	26	20
35 h	$\alpha + \beta_E + (TiCr_2)$	26	17
72 h	$\alpha + (TiCr_2)$	—	Nil
168 h	$\alpha + (TiCr_2)$	—	Nil
336 h	$\alpha + (TiCr_2)$	—	Nil
504 h	$\alpha + (TiCr_2)$	—	Nil
672 h	$\alpha + (TiCr_2)$	—	Nil

* Phases present listed in order of estimated quantitative proportions.

As decomposition progressed, a decrease in height of the initial sharp 7.26% Cr α (β_o) reflections was accompanied by the appearance and growth of broad, fuse, enriched beta (β_E) reflections. β enrichment at 420°C reached 26% Cr in two

TABLE II

X-RAY DIFFRACTION DATA OBTAINED FROM Ti–7.26% Cr ALLOY AGED AT 500°C

Ageing time	*Phases present*[a]	*% β_E Cr content (approx.)*	*% β_E (approx.)*
5 min	$\beta_o + \omega + (\alpha)$?	—	—
30 min	$\alpha + \beta_E + \omega$	—	—
1 h	$\alpha + \beta_E$	21	36
2 h	$\alpha + \beta_E$	21	36
6 h	$\alpha + \beta_E$	21	36
10 h	$\alpha + \beta_E + (TiCr_2)$	21	26
16 h	$\alpha + (TiCr_2) + (\beta_E)$	—	5
24 h	$\alpha + (TiCr_2)$	—	Nil
168 h	$\alpha + (TiCr_2)$[b]	—	Nil
336 h	$\alpha + TiCr_2$	—	Nil
504 h	$\alpha + TiCr_2$	—	Nil
672 h	$\alpha + TiCr_2$	—	Nil

[a] Phases present listed in order of estimated quantitative proportion.
[b] Formation of $TiCr_2$ peaks is apparent, but incomplete at this stage.

stages corresponding with ω- and α-phase formation, and at 500°C, reached 21% Cr.

There was no microscopic evidence of $TiCr_2$ precipitation at 420°C on ageing up to 672 h, nor was any positive identification made by X-ray diffraction. However, the ratemeter trace showed a very broad, weak peak (which for convenience will be referred to as $(TiCr_2)$) extending from about $2\theta = 42°–45.5°$, covering the positions of the strongest $TiCr_2$ reflections, the (311) and (222), after 35 h at temperature. Measurements of total counts in the range $2\theta = 41.5–46.5°$ showed a progressive increase to a maximum at 72 h which remained unchanged on further ageing (Fig. 1, curve A). No decrease in Cr content of β_E accompanying development of the broad

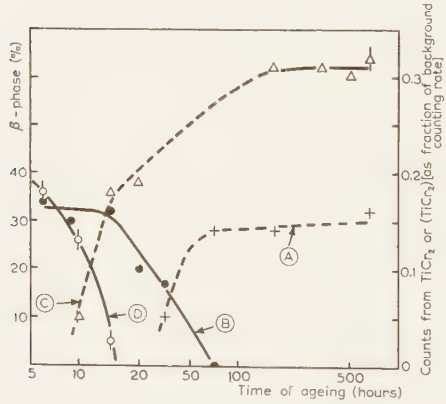

Fig. 1. Quantitative measurements of β_E and $TiCr_2$ contents *vs.* time of ageing (Ti–7.26% Cr alloy): A, $(TiCr_2)$ content, ageing temperature 420°C; B, β_E content, ageing temperature 420°C; C, $TiCr_2$ and $(TiCr_2)$ content, ageing temperature 500°C; D, β_E content, ageing temperature 500°C. In curve C, dotted line is indicative of $(TiCr_2)$ and full line of positively identified $TiCr_2$. (Statistical relative probable errors are indicated by appropriate range lines.)

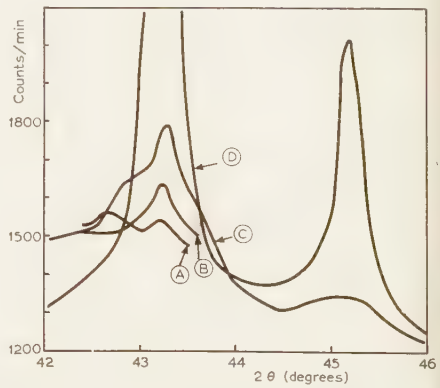

Fig. 2. Typical line profiles in the region 42–46° 2θ (Ti–7.26% Cr alloy): A, aged for 72 h at 420°C; B, aged for 672 h at 420°C; C, aged for 24 h at 500°C; D, aged for 672 h at 500°C. (The mean σ for curves A and B is 20 counts/min and for C and D, 60 counts/min.)

eflection was detected, and β_E disappeared by the time of its full development (Fig. 1, curve B).

More precise investigation of this peak was difficult because of its low intensity. caling techniques were used but a compromise was necessary between statistical ccuracy and the time required for making measurements. However, it was possible to how that the broad peak was resolved into two separate peaks after 72 h at tempera- ure. One was present at 42.8° 2θ and a somewhat weaker peak at 43.2° 2θ (Fig. 2, urve A). The latter is the position of the strong (311) $TiCr_2$ reflection, and after rolonged ageing, this peak only was obtained (Fig. 2, curve B). There was no evidence f the (222) $TiCr_2$ reflection even after 672 h ageing.

Somewhat similar features resulted from ageing at 500°C. At this temperature, owever, the ($TiCr_2$) reflection first appeared after 10 h ageing, and after 24 h in- ased to a level slightly higher than that reached in 672 h at 420°C together with a ore positive indication of the (222) reflection. Further ageing, to 168 h, resulted in evelopment of strong peaks characteristic of cubic $TiCr_2$. Full development of these, companying the disappearance of the ($TiCr_2$) reflection, occurred between 168 and 36 h (Fig. 1, curve C). No further change in X-ray patterns occurred on continued eing, suggesting that equilibrium had been attained. Metallographic identification f $TiCr_2$ was also established after 168 h, the phase being present as a dispersion of mall, dark etching particles. β_E disappeared prior to full development of the ($TiCr_2$) eflection (Fig. 1, curve D). Curves C and D of Fig. 2 show the line profiles obtained by he scaling technique after 24 and 672 h respectively.

Diffraction photographs of needle specimens showed preferred orientation maxima n the reflections from α, enriched β and $TiCr_2$ phases. In the samples examined, eflections from the latter two phases were quite weak, and that corresponding with $TiCr_2$) in the ratemeter trace was never observed. (110) enriched β was parallel to 0001) α and (311) $TiCr_2$ was parallel to (0001) α.

Lattice parameter measurements of the α-phase precipitated on ageing at both 20°C and 500°C showed no significant variation and agreed closely with reported alues for unalloyed Ti. In the 3.87% Cr alloy, the initial martensitic α parameter ecreased to that of unalloyed Ti after less than 30 min ageing at 500°C, and remained t this value throughout the course of continued ageing.

The α reflections from structures containing both ω- and α-phases were very iffuse. Measurements of width at half height of the (211) α reflection showed it to ecrease rapidly to a steady value following the disappearance of the ω-phase and overing the period of existence of the ($TiCr_2$) trace. A further sharpening of the eflections corresponded with the development of identifiable $TiCr_2$ at 500°C.

Hardness decreased during the period of ($TiCr_2$) precipitation and up to the time of ositive $TiCr_2$ precipitation, after which only a slight decrease occurred on prolonged eating. Ductility, however, as determined qualitatively in bend tests on specimens ged at 500°C, could be related to the structural changes detected by X-ray diffrac- ion. Whilst all specimens failed in a brittle manner, degrees of embrittlement as ndicated by deformation adjacent to the fracture surfaces were clearly apparent. o ductility was associated with structures containing ω-phase. Specimens in which he α- and β-phases only were detected showed some ductility, but this decreased ust prior to $TiCr_2$ detection. Ductility again improved as $TiCr_2$ precipitated, and mproved further with continued ageing.

DISCUSSION

The results show that at no stage in the course of β decomposition does the matrix consist entirely of the α-phase. Further, there is no evidence from lattice parameter measurements of an α-phase of high Cr content. While this does not necessarily disprove the existence of such a phase, it can be concluded that if it is, in fact, present the amount must be insufficiently large for detection by the technique used.

While it follows that $TiCr_2$ must be precipitated from enriched β, the evidence suggests that it is not precipitated directly, but is preceded by a transition stage as indicated by the broad reflection in the ratemeter trace and by changes in ductility. Although the possibility of this reflection being due to very finely-divided $TiCr_2$ cannot be rejected, its resolution into two minor but distinct peaks at 42.8° 2θ and 43.2° 2θ supports the existence of a distinct transition phase. Considering the results obtained after prolonged ageing at 420°C, it is possible that the presence of a single peak at 43.2° 2θ may be indicative of $TiCr_2$ precipitation, but of a particle size too fine for detection of the weaker (222) reflection. On this basis, it must be concluded that the peak at 42.8° 2θ is due to the transition phase which will be designated γ' for convenience.

There were insufficient data to indicate the nature of the γ'-phase. No other reflections attributable to it were detected. 42.8° 2θ corresponds with the position of the strong (110) reflection of a b.c.c. β-phase with a Cr content of about 70%. However, the existence of β enriched to this extent is unlikely, as formation of $TiCr_2$ would then occur by lattice adjustment without involving a eutectoid reaction in the original β decomposition sequence. While there is clearly danger in speculation, it is suggested that γ' is of similar composition to $TiCr_2$ and that $TiCr_2$ forms from it by a lattice adjustment. This would imply that the true eutectoid decomposition, resulting in α and γ', occurs considerably earlier than indicated by the appearance of $TiCr_2$. On the other hand, while there were short periods of coexistence of β_E and γ', there was no evidence of a decrease in Cr content of the β_E accompanying γ' precipitation. Strain in the α-phase at this stage of the decomposition sequence could possibly be attributed to coherency with the γ'.

While some differences with respect to reaction times between quenched and reheated, and corresponding isothermally quenched specimens are to be expected, there were major differences between the times in the present work, and those shown in the C-curves of FROST *et al.* and ROSTOKER for similar alloy compositions, isothermally quenched. In particular, in the present work, there was no coexistence of β-phase with identifiable $TiCr_2$, and there is some doubt as to whether $TiCr_2$ was formed at 420°C even after 672 h ageing.

The discrepancies may be attributed largely to the greater sensitivity of the X-ray technique used in the present case. In particular, the existence of γ' as proposed above may contribute to confusion in the early detection of $TiCr_2$. The phase is not visible microscopically and its X-ray reflection, even if observed by film techniques, may, because of its diffuse nature and proximity to the positions of $TiCr_2$ reflections, be mistakenly identified as $TiCr_2$. For the ageing temperatures under discussion, the inadequacy of metallographic examination for detection of phase changes would in any case necessitate use of X-ray techniques.

Further work is necessary to substantiate the existence of γ', to reveal its nature, and to determine whether its formation is dependent on temperature and the pres-

e of impurities. Its proposed existence, however, is not inconsistent with the mode $TiCr_2$ precipitation observed metallographically.

ACKNOWLEDGEMENTS

is paper is published by permission of the Chief Scientist, Australian Defence ientific Service, Department of Supply, Melbourne, Australia. The authors acknowlge with thanks helpful discussions with Mr. P. C. HUGHES, D.S.L., and Dr. W. A. CHINGER of the Aeronautical Research Laboratories.

REFERENCES

H. POLONIS AND J. G. PARR, *Trans. AIME*, 206 (1956) 531; Discussion, *J. Metals*, 9 (1957) 4.
I. AARONSON, W. B. TRIPLETT AND G. M. ANDES, Discussion, *Trans. Met. Soc. AIME*, 212 1958) 424.
H. KEYS, I. R. LAMBORN AND G. G. MCDONALD, *J. Inst. Metals*, 88, 4 (1959–60) 168.
D. FROST, W. M. PARRIS, L. L. HIRSCH, J. R. DOIG AND C. M. SCHWARTZ, *Trans. Am. Soc. Metals*, 46 (1954) 231.
V. ROSTOKER, Discussion, *Trans. Am. Soc. Metals*, 46 (1954) 251.
I. I. AARONSON, W. B. TRIPLETT AND G. M. ANDES, *Trans. Met. Soc. AIME*, 209 (1957) 1227.

RELATIONSHIPS BETWEEN IMPACT AND LOW-STRAIN-RATE HYDROGEN EMBRITTLEMENT OF TITANIUM ALLOYS*

D. N. WILLIAMS AND R. I. JAFFEE

Metallurgy Department, Battelle Memorial Institute, Columbus, Ohio (U.S.A.)

(Received April 13th, 1960)

SUMMARY

Hydrogen embrittlement of titanium alloys is generally separated into two types: impact embrittlement, which occurs in alpha–titanium alloys, and low-strain-rate embrittlement, which occurs in alpha–beta alloys. Data are presented which show that either low-strain-rate embrittlement or impact embrittlement can occur in alpha-compound, alpha–beta, or beta alloys depending on alloy composition and hydrogen content. These results suggest that both types of embrittlement are different manifestations of the same basic embrittling process, the rejection of hydride from solution in titanium, and that the type of embrittlement observed is related to the kinetics of hydride rejection. If hydride precipitates rapidly, impact embrittlement is observed. If hydrogen is held in supersaturation, strain-induced precipitation leads to low-strain-rate embrittlement.

INTRODUCTION

The ability of hydrogen to embrittle titanium alloys is generally considered to be separable into two distinct catagories: impact embrittlement and low-strain-rate embrittlement. The first is troublesome chiefly in alpha alloys, and is characterized by loss of strength in fast-strain-rate loading and increased notch sensitivity as hydrogen content increases. The second is a serious problem in alpha–beta alloys, and is characterized by embrittlement under low-strain-rate loading conditions, or, in extreme cases, from the presence of unrelieved residual stresses. This has led to the assumption that the two types of embrittlement are completely independent, and that each is restricted to one specific alloy type: impact embrittlement to alpha alloys and low-strain-rate embrittlement to alpha–beta alloys.

As information on the effects of hydrogen in titanium alloys has increased, it has become apparent that this generalization is untrue. It is the purpose of this paper to summarize some of the more recent findings to show first, that the two types of embrittlement are less restricted by alloy type than is generally supposed, and second, that impact and low-strain-rate embrittlement are closely related to each other, the observed differences in embrittlement behavior resulting from differences in the kinetics of precipitation of hydride in titanium alloys.

* This research was sponsored in whole or in part by the United States Air Force under Contract AF 33(616) 5007 monitored by the Materials Laboratory, Wright Air Development Center, Wright Patterson Air Force Base, Ohio.

LOW-STRAIN-RATE EMBRITTLEMENT IN ALPHA-COMPOUND ALLOYS

pha-compound alloys consist of a dispersion of a compound phase in an alpha atrix. Since low-strain-rate embrittlement has been considered to result from hyogen contained in the beta phase, it should not occur in alpha-compound alloys. ata on the effects of hydrogen in three alpha-compound alloys are given in Table I.

TABLE I

PROPERTIES OF THREE ALPHA-COMPOUND ALLOYS[1,2]

Titanium – 4 Aluminum – 7 Copper				
drogen content, p.p.m.	20	200	600	800
tched impact properties at				
77°F (in.-lb.)	6	10	—	4
nsile properties at 75°F				
(tested at 0.005 in./min)				
Ultimate strength, p.s.i.	141,000	146,800	—	153,200
Reduction of area, %	23	35	—	24
notched stress rupture properties				
at 75°F				
Stress, % of tensile strength	97	95	—	95
Time to failure, hours	5.6	> 310.9	—	17.8
Reduction of area, %	25	did not fail	—	8
otched stress rupture properties at 75°F				
Stress, % of tensile strength	—	110	110	110
Time to failure, hours	—	> 142.8	52.1	26.3
Reduction of area, %	—	did not fail	1.5	0.9
Titanium – 12 Tin – 7 Copper				
drogen content, p.p.m.	20	200	400	800
otched impact properties at				
77°F (in.-lb.)	8	8	—	—
nsile properties at 75°F				
(tested at 0.005 in./min)				
Ultimate strength, p.s.i.	149,700	145,000	—	—
Reduction of area, %	36	30	—	—
nnotched stress rupture properties at 75°F				
Stress, % of tensile strength	95	95	—	—
Time to failure, hours	1.1	> 316.8	—	–
Reduction of area, %	33	did not fail	—	—
otched stress rupture properties at 75°F				
Stress, % of tensile strength	—	110	110	110
Time to failure, hours	—	> 100.3	> 100.1	19.4
Reduction of area, %	—	did not fail	did not fail	1.3
Titanium – 7 Copper				
ydrogen content, p.p.m.	20	200	400	800
otched impact properties at				
77°F (in.-lb.)	20	—	5	—
nsile properties at 75°F				
(tested at 0.005 in./min)				
Ultimate tensile strength, p.s.i.	92,400	93,700	—	—
Reduction of area, %	40	48	—	—
nnotched stress rupture properties at 75°F				
Stress, % of tensile strength	95	—	—	—
Time to failure, hours	4.6	—	—	—
Reduction of area, %	41	—	—	—
otched stress rupture properties at 75°F				
Stress, % of tensile strength	—	—	110	110
Time to failure, hours	—	—	> 99.3	> 114.3
Reduction of area, %	—	—	did not fail	did not fail

It is apparent that two of these — Ti–4 Al–7 Cu and Ti–12 Sn–7 Cu — do show low-strain-rate embrittlement. This is demonstrated by the appreciable decrease of notched rupture life at 800 p.p.m. in both alloys. Ti–4 Al–7 Cu also shows some embrittlement in notched rupture testing at 600 p.p.m. and in unnotched rupture and tensile tests at 800 p.p.m. The third alloy — Ti–7 Cu — showed no evidence of low-strain-rate embrittlement, but impact embrittlement was observed.

Since none of these alloys contains beta, embrittlement may be assumed to result from some change in the alpha phase. Both 4 aluminum and 12 tin are completely soluble in alpha. It would appear, therefore, that these elements dissolved in alpha alter the alloy in such a way that it is susceptible to low-strain-rate embrittlement. The most obvious cause for such a change would be an increased ability to dissolve hydrogen, and to prevent its precipitation as hydride. The fact that Ti–7 Cu shows impact embrittlement which is known to result from the presence of hydride supports this assumption.

LOW-STRAIN-RATE EMBRITTLEMENT IN ALPHA ALLOYS

If aluminum and tin can render alpha-compound alloys susceptible to low-strain-rate embrittlement, it might be anticipated that Ti–Al and Ti–Sn alpha alloys would also be susceptible to low-strain-rate embrittlement. It is known that a Ti–5 Al alpha alloy shows a much higher solubility for hydrogen than unalloyed titanium[3]. The behavior of this alloy in notched stress rupture testing is shown in Table II. These data suggest that low-strain-rate embrittlement is occurring at 300 and 450 p.p.m.

TABLE II

PROPERTIES OF A TITANIUM-5 ALUMINUM ALPHA ALLOY[2,3]

Hydrogen content, p.p.m.	20	150	300	450
Notched impact properties at 75°F (in.-lb.)	39	39	4	4
Unnotched tensile properties (tested at 0.005 in./min)				
Ultimate tensile strength, p.s.i.	94,000	104,500	104,500	107,000
Reduction of area, %	37	36	23	16
Notched stress rupture properties at 75°F				
Stress, % of tensile strength	110	110	110	110
Time to failure, hours	> 221.2	> 213.5	111.1	177.2
Reduction of area, %	did not fail	did not fail	3.6	3.5

hydrogen. In addition, examination of the unbroken rupture test specimen containing 150 p.p.m. hydrogen showed that hydride precipitation had occurred under the notch during stress-rupture exposure, as shown in Fig. 1. It would appear, therefore, that the alloy is not at equilibrium at room temperature, being supersaturated with hydrogen. At 300 and 450 p.p.m. at least part of the hydrogen has precipitated as hydride, causing impact embrittlement. However, sufficient hydrogen in excess of the soluble amount apparently still remains to lead to susceptibility to low-strain-rate embrittlement. Low-strain-rate embrittlement has also been observed in a Ti–5Al–2.5 Sn alloy (A110AT) at 275 p.p.m. in unnotched stress rupture tests[4].

These data strongly suggest that low-strain-rate embrittlement is caused by precipitation of hydride under strain from an alpha alloy supersaturated in hydrogen.

(Magnification, 500 ×)

1. Strain-induced hydride near notch in titanium–5 aluminum alloy containing 150 p.p.m. rogen-rupture specimen stressed 213.5 hours without failure (2.77 reduction of area). Dark gray needles are hydride (see arrows).

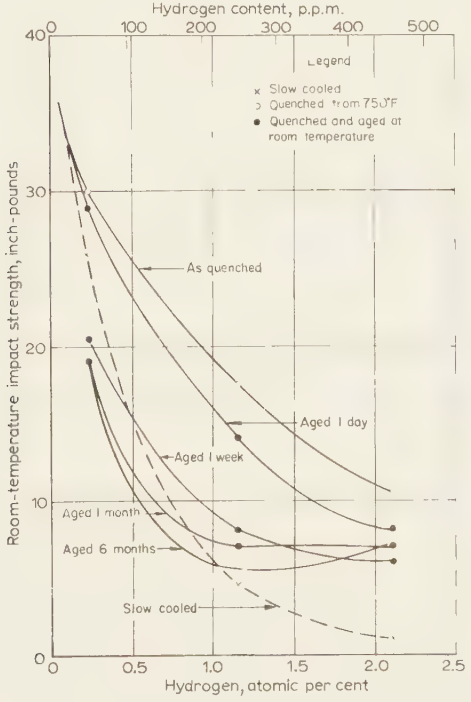

2. Effect of solution treatment and room temperature acting on the notch-bend impact strength of commercial A-55 titanium[5].

Quenched samples of unalloyed titanium are known to show progressive loss of impact properties if tested at increasingly longer times after quenching, as shown in Fig. 2. This suggests that hydrogen may remain in supersaturation in unalloyed titanium for short periods of time. If so, samples tested immediately after quenching might show low-strain-rate embrittlement. The results of an investigation to check this possibility are shown in Table III. No evidence of low-strain-rate embrittlement was observed. (Low-strain-rate embrittlement would be indicated if the ductility in slow speed tests were appreciably lower than that in fast speed tests.) Instead, samples quenched from both 800°F and 1675°F show a suggestion of impact embrittlement, being less ductile in fast speed tests, in agreement with the data shown in Fig 2. Therefore, it may be concluded that the explanation of the data shown in Fig. 2 offered in the original study was correct[5]. That is, that hydride precipitates on quenching as fine particles, which tend to coalesce with time.

TABLE III

VARIATION OF UNNOTCHED TENSILE PROPERTIES OF UNALLOYED TITANIUM (A-55) WITH HEAT TREATMENT AND STRAIN RATE[2] (SAMPLES TESTED IMMEDIATELY AFTER HEAT TREATMENT)

Heat treatment	*Strain rate (in./in./min)*	*Ultimate tensile strength (p.s.i.)*	*Reduction of area (%)*
	20 p.p.m. Hydrogen		
1 h at 1475°F, air-cooled	0.005	70,600	57
1/4 h at 1650°F, quenched	0.005	69,600	69
1 h at 800°F, quenched	0.005	70,600	55
	400 p.p.m. Hydrogen		
1 h at 1675°F, air-cooled	0.005	73,200	54
1 h at 1675°F, quenched	0.005	73,300	54
1 h at 1675°F, quenched	0.5	84,300	39
1 h at 800°F, quenched	0.005	75,000	58
1 h at 800°F, quenched	0.5	83,600	53

LOW-STRAIN-RATE AND IMPACT EMBRITTLEMENT IN BETA ALLOYS

Since low-strain-rate embrittlement has been shown to occur in alpha and alpha-

TABLE IV

PROPERTIES OF A TITANIUM–20 MOLYBDENUM BETA ALLOY[2]

Hydrogen content, p.p.m.	20	800	3,000	3,600	4,200
Notched impact properties at 75°F (in.-lb.)	8	6	—	—	—
Unnotched tensile properties at 75°F (tested at 0.5 in./min)					
Ultimate tensile strength, p.s.i.	142,100	143,400	146,500	148,000	150,000
Reduction of area, %	43	38	39	32	5
Unnotched tensile properties at 75°F (tested at 0.005 in./min)					
Ultimate tensile strength, p.s.i.	136,400	136,800	133,000	134,000	136,500
Reduction of area, %	37	36	28	11	0
Notched stress rupture properties at 75°F					
Stress, % of tensile strength	110	110	110	110	80
Time to failure, hours	> 206.9	> 216.7	0.1	9.8	4.2
Reduction of area, %	did not fail	did not fail	5.0	1.1	0.7

mpound alloys, as well as alpha–beta alloys, it is of interest to determine whether beta phase is of significance in the embrittlement process. Data have been obned on a titanium–20 molybdenum alloy, containing only a minute amount of eroidal alpha, which show that both impact and low-strain-rate embrittlement ur in a beta alloy. These data are given in Table IV.

ow-strain-rate embrittlement is apparent at 3,600 p.p.m. comparing tensile tests ducted at two strain rates, and at 3,000 p.p.m. in notched rupture tests. Impact rittlement (or possibly complete embrittlement) is apparent at 4,200 p.p.m. At 00 p.p.m. a notched rupture specimen loaded at 110% of the tensile strength failed h zero reduction of area on loading.

DISCUSSION OF RESULTS

a have been published previously showing that alpha–beta alloys exhibit impact rittlement approximately 100 p.p.m. higher in hydrogen content than the hydrogen tent resulting in low-strain-rate embrittlement[6]. Thus, depending on alloy comion, either impact or low-strain-rate embrittlement may occur in alpha, alpha-mpound, alpha–beta, and beta titanium alloys. Embrittlement is not a condition urring only in a certain type of alloy. Moreover, the observance of both types of rittlement in the same class of alloy, with differences in alloy composition or drogen content, suggests that the two types of embrittlement are closely related. he behavior described above can be explained if it is assumed that embrittlement both cases results from the presence of a hydride phase, and that the solubility ydrogen in both alpha and beta titanium decreases rapidly as room temperature pproached. If the hydride precipitates easily, it is present in the alloy at room perature, and the alloy shows impact embrittlement. If the rejection of hydride ot rapid, the alloy exists in a non-equilibrium supersaturated state at room temperc, leading to rejection of hydride during straining (or under the action of high idual stresses) with low-strain-rate embrittlement resulting.

he much larger amount of hydrogen required to embrittle beta alloys as compared h alpha alloys indicates either that the equilibrium solubility of hydrogen is ter in beta than in alpha titanium or that the sluggishness of the hydride rejection reater. Probably both factors are significant. It has been suggested that hydride not nucleate readily in beta titanium[7]. The alpha–beta interface in two phase ys may then serve as a site of easy nucleation, leading to the very marked senvity of alpha–beta alloys to low-strain-rate embrittlement. The alpha-compound rface may serve a similar purpose, as indicated in the data presented in this paper, ch showed embrittlement to be more drastic in Ti–4 Al–7 Cu than in Ti–5 Al. would also appear that the presence of thermally-precipitated hydride may serve a site for further hydride rejection, such that an alloy may show decreasing sustibility to low-strain-rate embrittlement as the hydrogen content increases to a nt sufficiently beyond the solubility limit to prevent complete retention of hygen in solution. This trend is seen in the notched stress rupture results for the 5 Al alloys at 300 and 450 p.p.m. in Table II and has been reported previously a Ti–4 Mn alpha–beta alloy[1].

Although hydrogen embrittlement is a universal trait of titanium alloys, it is of le practical significance in most cases since the hydrogen content necessary to

induce embrittlement is too high. Thus, impact embrittlement is a serious problem only in unalloyed alpha titanium where hydrogen solubility is low and rejection of hydride is rapid, while low-strain-rate embrittlement is a serious problem only in those alpha–beta alloys showing low equilibrium solubility, a tendency toward supersaturation, and ample nucleation sites for strain-induced hydride precipitation.

REFERENCES

1 D. N. WILLIAMS, F. R. SCHWARTZBERG, P. R. WILSON, W. M. ALBRECHT, M. W. MALLETT AND R. I. JAFFEE, Hydrogen contamination in titanium and titanium alloys, Part IV: The effect of hydrogen in titanium alloys, *WADC Technical Report 54-616*, Part IV, March, 1957.

2 D. N. WILLIAMS, F. R. SCHWARTZBERG AND R. I. JAFFEE, Hydrogen contamination in titanium and titanium alloys, Part V: Hydrogen embrittlement, *WADC Technical Report 54-616*, Part V, March, 1958.

3 L. W. BERGER, D. N. WILLIAMS AND R. I. JAFFEE. Hydrogen in titanium–aluminum alloys, *Trans. A.I.M.E.*, 212 (1958) 509.

4 D. R. LUSTER, *Mechanical Metallurgy, II-Ductility*, New York University Titanium Metallurgy Course, Lecture No. 17, September 13, 1956.

5 G. A. LENNING, C. M. CRAIGHEAD AND R. I. JAFFEE, Constitution and mechanical properties of titanium–hydrogen alloys, *Trans. A.I.M.E.*, 200 (1954) 357.

6 R. I. JAFFEE AND D. N. WILLIAMS, The effect of composition on the hydrogen embrittlement of alpha–beta titanium alloys, *Trans. Am. Soc. Metals*, 51 (1959).

7 A. D. MCQUILLAN, *Hydrogen in Titanium and Its Alloys*, New York University Titanium Metallurgy Course, Lecture No. 11, September 12, 1956.

COMPLEX COMPOUNDS OF INDIUM TRIHALIDES PART I. ETHER COMPLEXES

FRED FAIRBROTHER, NEVILLE FLITCROFT AND HAROLD PROPHET

(Department of Chemistry, The University of Manchester, England)

(Received May 9th, 1960)

SUMMARY

Complex compound formation between indium trichloride, tribromide and triiodide, and a number of ethers has been examined. Twenty-three systems were examined and in all but three complex formation was observed, twenty-five definite compounds being identified. An outstanding feature was the widespread formation of 1 : 2 complexes, in contrast to the behaviour of the trihalides of other members of this group, which form predominantly 1 : 1 complexes.

In all cases indium trichloride dissolves in an ether very slowly, even when the ultimate solubility is high. This is correlated with an energy of re-organization of the ionic solid to form a molecular complex. Stereochemical considerations affect the complexing powers of the different ethers.

INTRODUCTION

Many compounds of ethers with the trihalides of boron, aluminium and, to a less extent, with gallium have been described. In contrast, the investigation of the corresponding compounds with indium trihalides has been almost completely neglected. This has sometimes led to the belief that such compounds do not exist. The absence of studies in this field may possibly be due to the fact that, on casual observation, indium trichloride is insoluble in ethers such as diethyl ether, dioxan or tetrahydrofuran. Nevertheless it forms soluble stable compounds with all these ethers. When I began this work, only one trihalide ether complex, $InBr_3,2$(1 : 4-dioxan) had been reported[1], prepared incidental to the main investigation by the addition of dioxan to an ether solution of the halide. Since then another, alleged to be $InBr_3,(C_2H_5)_2O$, has been cited[2], but we find no evidence for its existence. We have now examined the indium trihalide ether systems in which 25 definite complexes were identified, either by phase studies or chemical analysis of the crystalline adducts, or both. We have also examined complexes formed between these halides and a number of thioethers. These will form the subject of a separate communication.

Some years ago[3] a preliminary investigation in these laboratories indicated that indium trichloride and tribromide formed dietherates with ethyl ether, of empirical formulae $InCl_3,2(C_2H_5)_2O$ and $InBr_3,2(C_2H_5)_2O$. The present work has indicated that the formation of such di-etherates of indium trihalides is widespread and in contrast to experience with the trihalides of other members of this group, which form chiefly mono-etherates.

EXPERIMENTAL

Indium trichloride was prepared by heating high-purity indium at 450° in a stream of dry chlorine. Repeated vacuum sublimation at 420° gave a white crystalline product which left no residue and which was sublimed in a vacuum into fragile hook-ended ampoules. Typical analyses were: Found: In, 52.13; Cl, 48.11%; In, 52.00; Cl, 47.86%; In, 52.24; Cl, 47.87%; $InCl_3$ requires In, 51.90; Cl, 48.10%. Indium tribromide was prepared in a similar manner by heating the metal at 400° in a bromine-saturated stream of nitrogen followed by fractional sublimation *in vacuo* at 280°. Typical analyses were: Found: In, 31.85; Br, 67.72%; In, 32.30; Br, 67.54%; $InBr_3$ requires In, 32.34; Br, 67.66%.

Indium triiodide was prepared by heating the metal with excess (10%) iodine at 200° for about 24 h in a sealed tube. Most of the excess iodine, the presence of which was necessary to prevent the formation of lower iodides, was removed by heating one end of the tube at 150° and cooling the other in a current of air. Fractional vacuum sublimation gave a bright yellow product, which was, likewise, stored in fragile hook-ended ampoules. Typical analyses were: Found: In, 23.00; I, 76.89%; In, 22.86; I, 76.99%; In, 23.41; I, 76.88%. InI_3 requires In, 23.15; I, 76.85%.

Dimethyl ether: The commercial cylinder-product was condensed at —78° on to lithium aluminium hydride and roughly fractionated in a closed system. The middle fraction was adsorbed, for use, on to fine-mesh silica gel which had been degassed at 300°. Diethyl-, di-*n*-butyl, di-isopropyl and di-isoamyl ethers, tetrahydrofuran, 1:4-dioxan and 2-methyl-tetrahydrofuran: commercial products were purified by the usual methods, dried by refluxing with sodium metal, fractionated and stored over bright sodium wire in an atmosphere of nitrogen.

2:5-dimethyltetrahydrofuran was prepared from commercial hexane-2:5-diol by boiling with potassium pyrosulphate by the method of REPPE[4] and was purified, dried and stored in a similar manner.

Vapour pressure/composition measurements were carried out by the method described elsewhere[5]. For systems involving dimethyl ether, the water thermostat was replaced by a large well-lagged Dewar-flask containing a well-stirred slush of melting chloroform (—63.5°), cooling being maintained by a "finger" filled with solid carbon dioxide. For this ether also, the usual measuring burette was replaced by a tube containing dimethyl ether adsorbed on to silica gel. This tube, by a system of taps and ground joints, could be removed from the apparatus, weighed and restored to the reaction system, without ingress of moisture or air or loss of ether.

Direct solubility measurements. These were carried out either in sealed tubes by the "disappearing crystal" method or by saturation in an all-glass sealed apparatus using the technique described by FAIRBROTHER, SCOTT AND PROPHET[6]. The final stage of drying in the latter method was carried out by condensing the ethers on to lithium aluminium hydride prior to evaporation into the solubility cell. In every case, at the end of a completed run, a small amount of ether was distilled from the solubility cell and its infra-red absorption spectrum compared with that of the pure solvent. This established that no "splitting" of the ether had occurred. Since the solid phase in equilibrium with the saturated solution was, according to the system, uncomplexed halide or complex containing one or two molecules of ether, the results are recorded uniformly in terms of grams halide dissolved in 100 g ether.

Condensed systems were also examined by the usual methods of thermal analysis. ie apparatus consisted simply of a pyrex tube (3 in. × ½ in.) sealed at one end and ted with a B14 socket at the other. This socket was provided with a well-fitting opper through which passed the stem of a thermometer graduated in 1/10°. The pper end of the thermometer fitted loosely into an off-centre hole in a small hori- ntal wooden disc, rotated slowly by a constant-speed motor. The rubber stopper s sufficiently flexible to allow the thermometer to act also as stirrer. The glass be, surrounded by a wider one was immersed in a large beaker containing glass bol, ice-water or acetone–solid CO_2 according to the temperature range under in- tigation. Systems were examined by introducing weighed amounts of the com- ients into the inner tube, under a nitrogen cover, warming until a homogeneous lution was obtained and then observing the cooling curve in the appropriate sur- undings.

RESULTS

stem indium trichloride–dimethyl ether

At a temperature of —35°, which was conveniently below the boiling point at mospheric pressure, no complex formation could be observed. Using a mole ratio, $_2O/InCl_3$ of 20:1 at —35°, no dissolution of the halide could be detected even ter four days. Since ready complex formation was observed between this ether and er trihalides and since dissolution of indium trichloride in diethyl ether (see below) s extremely slow, it was felt that this failure might be due to the low temperature which it was necessary to work in simple glass apparatus.

Accordingly, 2.1 g trichloride (~0.01 mole) was transferred under a nitrogen cover a glass tube which was then enclosed in a stainless steel pressure vessel of about 0 ml capacity. This vessel was evacuated and about 75 ml of dimethyl ether con- nsed on to the halide by cooling at —195°. The needle valve on the pressure vessel s closed and the temperature allowed to rise to room temperature with a corre- onding rise of pressure to 4–5 atmospheres. The vessel was then shaken for 7 days this temperature and attached to the vapour pressure apparatus in place of the ual reaction vessel. Both vapour pressure measurements and analysis of the residue the tube showed that a complex, $InCl_3,2(CH_3)_2O$, had been formed. [Found: , 37.10; Cl, 33.99%. $InCl_3,2(CH_3)_2O$ requires In, 36.65; Cl, 33.95%.]

Measurements of the dissociation pressure of the solid complex, at five temperatures om 20.6° to 39.3° gave an approximate value of $\Delta H = -19.9$ kcal.mole^{-1} for the action:

$$InCl_{3(c)} + 2(CH_3)_2O_{(g)} \rightarrow InCl_3,2(CH_3)_2O_{(c)}$$

stem indium trichloride–diethyl ether

It was observed, in all experiments with this system, that at room temperature e indium trichloride dissolved in the ether very slowly indeed, 24 hours with con- uous shaking usually being necessary for complete dissolution. On the other hand, cooling a sufficiently concentrated solution to 0°, colourless hygroscopic crystals $InCl_3,2(C_2H_5)_2O$ were deposited. These were purified by recrystallization, m.p. 22°. ound: In, 31.26; Cl, 27.57%. $InCl_3,2(C_2H_5)_2O$ requires In, 31.09; Cl, 28.80%.]

The composition of this complex was confirmed by dissociation-pressure measurements. Runs were carried out at 0°, 15.8° and 23.4°. At all three temperatures the phase diagrams indicated the formation of a solid phase with the composition $InCl_3,2(C_2H_5)_2O$ with no evidence for the formation of a mono-etherate.

The equilibrium dissociation pressures at the three temperatures were respectively 5 mm, 22 mm, and 41 mm. These give an approximate value for the heat of the reaction:

$$InCl_{3(c)} + 2(C_2H_5)_2O_{(g)} \rightarrow InCl_3,2(C_2H_5)_2O_{(c)}$$

$$\Delta H = -33.5 \text{ kcal.mole}^{-1}$$

By assuming that each molecule of $InCl_3$ had prevented two molecules of ether from functioning as solvent, the depression of the vapour pressure above homogeneous unsaturated solutions gave values for the molecular weight of the solute such as 426, 439, 420, 439; Calc. for $InCl_3,2(C_2H_5)_2O$, mol. wt. = 369.5. This indicates that the species present in solution was largely the di-etherate of the monomer $InCl_3$.

Solubility breaks were observed at mole per cent $InCl_3$ of 24.2 and 30.3 at 0° and 15.8°, respectively. Direct measurements of the solubility by the "disappearing-crystal" method gave:

t°	Mole % $InCl_3$	s (g $InCl_3$/100 g diethyl ether)
−13.7	19.3	71.5
0.8	25.3	101.1
5.0	27.0	110.6
17.2	31.4	136.8
20.1	32.6	144.5

These values, plotted as log s against $1/T$ lie very close to a straight line, a very short (2°) extrapolation of which gives the m.p. of the complex as 22°.

The solubility is much higher than the 35.18 g/100 g ether at 20° reported by Ensslin and Lessmann[7], the divergence doubtless being due to the slowness with which equilibrium is established in this system.

*System indium trichloride–di-*n*-propyl ether*

Again, the rate of dissolution was extremely slow, but concentration of the solution and cooling to 0° gave colourless crystals of $InCl_3,2(n\text{-}(C_3H_7)_2O)$ m.p. approx. 10°. [Found In, 27.2; Cl, 26.5%. $InCl_3,2(n\text{-}(C_3H_7)_2O)$ requires In, 26.96; Cl, 25.0%.] The infra-red absorption spectrum of the liquid was quite different from that of the pure solvent.

*Systems indium trichloride–di-isopropyl, di-*n*-butyl and di-isoamyl ethers*

With none of these ethers was complex formation observed. Saturated solutions were obtained only after continuous agitation for several days and the infra-red spectra of the solutions saturated at room temperature were indistinguishable from those of the pure ethers. The solubilities are given in Table I.

System indium trichloride–tetrahydrofuran

Again, dissolution was extremely slow even at 40°, agitation for up to 24 h being

TABLE I

$t°$	Mole % $InCl_3$	s (g/100 g ether)
	isopropyl ether	
16.0	0.539	1.17
26.9	0.658	1.43
33.1	0.648	1.41
39.9	0.724	1.58
47.9	0.847	1.85
48.5	0.787	1.72
	n-*butyl ether*	
17.3	2.05	3.55
23.7	2.49	4.34
24.9	2.55	4.45
29.7	2.83	4.94
30.1	2.93	5.13
36.0	3.38	5.94
41.2	3.77	6.65
	isoamyl ether	
17.9	4.39	6.42
23.3	5.26	7.76
29.5	6.09	9.06
35.0	7.33	11.0
40.9	7.82	11.8

essary. Vapour pressure studies showed the existence of two complexes, $InCl_3$, H_8O and $InCl_3,2C_4H_8O$. The former has a relatively high dissociation pressure:

$t°$	p(mm)
21.5	27.7
23.5	32.7
25.7	38.5

ing for $InCl_3,2C_4H_8O_{(c)} + C_4H_8O_{(g)} \rightarrow InCl_3,3C_4H_8O_{(c)}$ $\Delta H = -13$ kcal.mole^{-1}. portion of the complex removed from the apparatus at the end of a series of solubility measurements melted at 50° and gave: In, 26.10; Cl, 24.02%; $InCl_3,3C_4H_8O$ uires In, 26.22; Cl, 24.31%.

The di-etherate, on the other hand, had a low dissociation pressure: 5.0 mm at ° and 12.4 mm at 30.0°. Long periods of pumping were required to attain the final mposition. [Found: In, 30.45; Cl, 28.99%. $InCl_3,2C_4H_8$ requires In, 31.42; Cl, 12%.] The complex melted at 98.5°–101°.

The depression of the vapour pressure in unsaturated solutions gave values of the lecular weight which corresponded more closely to a 1:2 complex than to a 1:3. s possible therefore that $InCl_3,3C_4H_8O$ exists only in the solid state and is of the ure of a lattice compound. The solubility of indium trichloride in tetrahydrofuran ve:

$t°$	Mole % $InCl_3$	s (g $InCl_3$/100 g tetrahydrofuran)
17.8	6.49	21.3
24.1	8.72	29.3
29.9	11.29	39.0
33.2	13.20	46.7

System indium trichloride–2 methyltetrahydrofuran

Removal of excess solvent, *in vacuo*, from a solution of the halide gave large (approx. 5 mm) white crystals of $InCl_3$,2(2-methyltetrahydrofuran) m.p. 47–48°. [Found: Cl, 26.68; C, 29.4; H = 5.1%. Complex requires: Cl, 27.05; C, 30.54; H, 5.1%.]

System indium trichloride–2: 5-dimethyltetrahydrofuran

In a similar manner, white crystals, m.p. 71° of $InCl_3$,2(2:5-dimethyltetrahydrofuran) were obtained. [Found: Cl, 25.45; C, 32.7; H, 5.3%. Complex requires: Cl, 25.24; C, 34.19; H = 5.74%.]

System indium trichloride–1: 4-dioxan

Although a very stable complex was ultimately formed, dissolution of the halide was very slow (and often required the system to be heated to nearly 100° for completion). On removal of excess solvent large (several mm) colourless, bi-refringent and probably triclinic, crystals of $InCl_3$,2(1:4-dioxan) were obtained. [Found: In, 28.01; Cl, 26.63%. $InCl_3$,2(1:4-dioxan) requires In, 28.88; Cl, 26.77%.]

The crystals could be handled in air and stored without undue precautions, being only slightly hygroscopic. The complex did not melt but observation in polarized light showed that decomposition began at about 90° and progressed until the crystals were quite opaque at 120°. The resulting solid, presumably $InCl_3$(1:4-dioxan) did not melt but underwent further decomposition in the region of 150°. Vapour pressure studies confirmed the existence of $InCl_3$,2(1:4-dioxan) and also of $InCl_3$,(1:4-dioxan). The dissociation pressures of the 1 : 2 complex were at 39.1°, 1.2 mm, at 69.0°, 6.1 mm, and at 81.0°, 8.65 mm, corresponding to a heat of reaction $InCl_3$, 1:4-dioxan$_{(c)}$ + 1:4-dioxan$_{(g)}$ → $InCl_3$,2(1:4-dioxan)$_{(c)}$ ΔH = —10.0 kcal.mole^{-1}. The complex $InCl_3$,1:4-dioxan was non-hygroscopic and stable *in vacuo* at 50°. [Found: In, 36.46; Cl, 34.88%. $InCl_3$,1:4-dioxan requires In, 37.11; Cl, 34.40%.] Solubility measurements by saturation gave:

$t°$	Mole % $InCl_3$	s (g/100 g 1:4-dioxan)
15.8	6.16	16.5
21.4	7.05	19.0
28.8	8.77	24.1
35.5	10.0	27.9
42.5	11.8	33.7
49.4	14.3	41.8

System indium tribromide–dimethyl ether

Dissolution occurred readily at —63.5°, giving a colourless solution which on eva-

ration deposited white crystals of a very hygroscopic complex $InBr_3,2(CH_3)_2O$ m.p. –87°. [Found Br, 53.09; C, 10.45; H, 2.35%. $InBr_3,2(CH_3)_2O$ requires Br, 53.68; 10.76; H, 2.6%.] The dissociation pressure of the complex at —63.5° was only 35 cm. In consequence, confirmation of this composition by vapour pressure measurements was difficult. The solubility at this temperature was approximately g $InBr_3$/100 g $(CH_3)_2O$.

stem indium tribromide–diethyl ether

Dissolution occurred rapidly, with evolution of heat. Vapour pressure measurements showed the formation of $InBr_3,2(C_2H_5)_2O$, with a dissociation pressure of 1.26 at 17.8°, and 1.36 cm at 19.6°, which decomposed directly to the trihalide without formation of a mono-etherate. The complex, which separated from a saturated tion was white and crystalline, m.p. 25°. [Found: In, 22.89; Br, 48.6%; $InBr_3$, $_2H_5)_2O$ requires In, 22.81; Br, 48.45%.] Direct measurements of the solubility gave:

t	*Mole %*	*s (g $InBr_3$/100 g diethyl ether)*
—19.0	21.0	127.2
—14.2	22.4	137.8
—10.5	23.2	144.5
5.1	27.6	182.5
14.6	30.5	209.8
25.0	33.3	239.2

stem indium tribromide–di-isopropyl ether

At a mole ratio of ether: halide even as dilute as 25:1 and on heating, dissolution curred only very slowly. Once dissolved, however, the tribromide showed itself to very soluble and no solid was deposited at room temperature up to a mole ratio 4:1. The system was studied by both the disappearing crystal technique and ermal analysis, which indicated the formation of a complex $InBr_3,2((CH_3)_2CH)_2O$, .p. approx. 41°, which was extremely deliquescent and decomposed rapidly in a cuum to $InBr_3$. Owing to the deliquescent nature of the solid, reliable analyses could t be obtained.

t°	*Mole % $InBr_3$*	*s (g $InBr_3$/100 g di-i-Pr_2O)*
—9.5	10.1	38.8
—5.5	11.6	45.4
—0.3	13.6	54.8
6.1	16.6	68.9
16.0	21.1	93.0
27.5	26.9	127.4
35.7	30.6	152.9

ystem indium tribromide–di-n-*butyl ether*

Dissolution occurred very readily and thermal analysis indicated the existence of a mplex $InBr_3,2(C_4H_9)_2O$, m.p. 18°. This again was very deliquescent and difficult to ndle for analysis. The temperatures at which solid phase appear were as follows:

$t°$	Mole % $InBr_3$	s (g $InBr_3$/100 g di-n-Bu_2O)
—15.8	15.7	50.7
— 7.2	17.5	57.9
— 1.4	19.9	67.5
6.3	22.9	80.3
14.0	27.0	100.8
16.0	28.7	109.7

System indium tribromide–tetrahydrofuran

Dissolution was rapid, to give a colourless solution from which white crystals were deposited. Three vapour pressure runs were carried out at temperatures around 24°. All of these indicated the formation of a stable crystalline complex, $InBr_3,2C_4H_8O$, with a very low dissociation pressure. [Found: In, 23.3; Br, 48.22%. $InBr_3,2C_4H_8O$ requires In, 23.03; Br, 48.1%.] Samples sealed in tubes with nitrogen gave m.p. 101–101.5°.

The values of the apparent molecular weight in unsaturated solution, derived from the depression of the vapour pressure agreed more closely with the composition $InBr_3,3(C_4H_8O)$ than with $InBr_3,2(C_4H_8O)$. It is possible therefore that some additional solvation of the complex occurs in solution, this being the converse of the results in the indium trichloride–tetrahydrofuran system in which the additional solvation is only found in the solid complex. Direct measurements of the solubility gave:

$t°$	Mole % $InBr_3$	s (g $InBr_3$/100 g tetrahydrofuran)
4.2	15.0	87.0
12.0	16.0	93.9
17.8	17.6	105.4
24.1	18.6	112.7

System indium tribromide–1:4-dioxan

Dissolution was fairly rapid at room temperature and almost instantaneous on gently warming. The system was investigated by the thermal analysis method which showed the formation of a complex $InBr_3,2C_4H_8O_2$, melting incongruently at 130.5–131.3. Large (4 mm) crystals could be grown by slow evaporation of a solution. These were bi-refringent and probably triclinic but with extinction angles not more than 10° from parallel, and were stable at room temperature. [A sample dried for 6 h, in a stream of nitrogen gave, In, 21.87; Br, 45.34%. $InBr_3,2C_4H_8O_2$ requires In, 21.62; Br, 45.18.] Thermal analyses gave the following figures:

t	Mole % $InBr_3$	s (g $InBr_3$/100 g 1:4-dioxan)	Eutectic
10.0	3.30	13.7	6.3°
9.5	4.09	17.2	6.3°
8.6	5.38	22.9	5.8°
8.2	6.39	27.6	5.8°
6.0	7.86	34.3	6.0°
21.5	8.89	39.3	5.3°
68.5	11.4	51.6	
97.0	12.5	57.6	

stem indium tribromide–1:2-dimethoxyethane

Again, at first, the halide appeared to be insoluble in this ether: 4 g failed to dissolve 30 ml ether during 3 days. On long standing and warming, however, a solution ntaining, at 25.8°, about 55 g $InBr_3$/100 g ether was obtained. A single determi- tion of the vapour pressure/composition relation at this temperature indicated the mation of the complex $InBr_3,2$(dimethoxyethane) with a dissociation pressure of 3 cm. Equilibrium was reached very slowly and it could not be ascertained whether urther compound $InBr_3$, dimethoxyethane was formed. This, however, can not be ely excluded since after continuous pumping of one specimen a solid with ap- oximately this composition was obtained: [Found. In, 24.16; Br, 53.95%. $InBr_3$, methoxyethane requires In, 25.82; Br, 53.93%.]

stem indium triiodide–dimethyl ether

Dissolution of the yellow halide occurred readily at —63.5° to give a colourless ution from which, on evaporation of the solvent, white very hygroscopic crystals the complex $InI_3,2(CH_3)_2O$, m.p. 38°, and dissociation pressure, at —63.5°, 0.45 cm. und: I, 64.73; C, 7.0; H, 1.6%. $InI_3,2(CH_3)_2O$ requires I, 64.80; C, 8.18; H, 24%. The low C,H values are due to the loss of ether at room temperature.]

The composition of the complex was also confirmed by vapour pressure measure- nts.

stem indium triiodide–diethyl ether

Again, dissolution was rapid, the bright yellow solid giving a colourless solution l colourless crystals of the complex $InI_3,(C_2H_5)_2O$, which could be purified by rystallization from the ether, m.p. 29°. [Found: In, 19.96; I, 66.95%. $InI_3,(C_2H_5)_2O$ quires: In, 20.14; I, 66.83%.] Measurements of the vapour pressure/composition tion at 19.4° confirmed this composition of the complex which at 19.4° had the y low dissociation pressure of 0.4 mm. Measurement of the dissociation pressure r a range of temperatures from 0°C (0.014 cm) to 54.5°C (0.378 cm) led to a heat formation of the complex.

$$InI_{3(c)} + (C_2H_5)_2O_{(g)} \rightarrow InI_3,(C_2H_5)_2O_{(c)}:$$

$$\Delta H = -10.7 \text{ kcal.mole}^{-1}$$

Thermal analysis of part of the condensed $InI_3,(C_2H_5)_2O$ system also confirmed s composition of the complex:

t°	Mole % InI_3	s (g InI_3/100 g diethyl ether)
—18.5	31.0	299.9
—11.8	33.7	339.8
— 5.8	35.7	371.4
4.8	39.0	426.9
17.0	44.8	541.8
23.2	47.8	612.0

stem indium triiodide–tetrahydrofuran

Rapid dissolution gave a colourless solution which deposited large white crystals

of the hygroscopic complex $InI_3,2C_4H_8O$. [Found: In, 17.22; I, 59.06; C, 14.7; H, 1.85%. $InI_3,2C_4H_8O$ requires: In, 17.93; I, 59.51; C, 15.02; H, 2.52%.] Vapour pressure measurements with this system proved very difficult, since in the concentrated region close to the mole ratio 1:2, equilibrium was only attained slowly. In consequence, no precise figures for the dissociation pressure, which varied between 0.3 cm and 0.5 cm at 23.5° can be given. The measurements, however, left no doubt that the composition of the complex was $InI_3,2C_4H_8O_2$. Direct measurements of the solubility gave the following:

t°	Mole % InI_3	s (g InI_3/100 g tetrahydrofuran)
12.1	14.1	113.0
18.9	15.1	122.2
26.1	16.9	139.3
32.6	18.2	152.6
39.2	19.7	169.0

System indium triiodide–di-isopropyl ether

Dissolution was fairly slow but more rapid than in the case of the tribromide. The colourless solution deposited white crystals which turned yellow on standing, presumably owing to loss of ether. Vapour pressure measurements at 24.72° and 69° indicated the existence of two complexes, $InI_3,2((CH_3)_2CH)_2O$ and $InI_3,(CH_3)_2CH)_2O$ the former melting at 84° and having a dissociation pressure of 0.120 cm at 24.72 and 2.68 cm at 69°. The dissociation pressure of the mono-etherate could not be measured. The complex is not very soluble in the ether, the approximate solubility at 24.72° being 14 g InI_3/100 g ether.

*System indium triiodide–di-*n*-butyl ether*

The triiodide dissolved easily to give a clear light-amber-coloured solution. Great difficulty was experienced with this system, either in obtaining a solid phase from solution or thermal analysis of the system, owing to the readiness of a concentrated solution to set into a glassy solid on cooling.

The system was examined by means of the disappearing crystal technique mixtures being prepared by concentrating a dilute solution and maintaining it for some hours at a temperature below saturation but above that at which it became glassy until solid appeared. In this way the phase diagram indicated the presence of two compounds, $InI_3,2Bu_2^nO$ melting at —8.85° and InI_3, Bu_2^nO melting at —11.3°.

The values of the apparent solubilities of InI_3 were as follows:

t°	Mole % InI_3	s (g InI_3/100 g Bu_2O)	Solid phase
—12.0	22.9	113.1	InI_3, 2,Bu_2O
—11.5	25.8	132.0	,,
—10.9	28.3	150.0	,,
— 9.8	30.8	169.6	,,
— 9.0	33.0	187.4	,,
— 9.0	34.8	203.3	,,
— 9.4	36.4	217.7	,,
—10.0	38.8	241.5	,,

$t°$	*Mole % InI_3*	*s (g InI_3/100 g Bu_2O)*	*Solid phase*
—11.9	40.0	254.2	,,
—14.0	41.5	270.4	,,
—14.6	43.0	286.7	eutectic
—13.4	46.9	336.2	InI_3 Bu_2O
—12.2	49.4	371.9	,,
—11.3	50.0	380.6	,,

stem indium triiodide–1:4-dioxan

Indium triiodide is not very soluble in dioxan and only dissolves at all quickly if ated. Examination of the system by thermal analysis proved difficult, chiefly ause the melting points of the complexes were above the boiling point of the xan, and mixtures generally tended to boil before solution was complete. By maining the air-thermostat around the apparatus at about 45°, it was possible to carry t vapour pressure measurements and in this way the existence of two stable white ystalline complexes which hydrolysed only slowly in air was established. (i) InI_3, 1:4-dioxan), dissociation pressure 3.8 cm at 39.1°. [Found: In, 15.01; I, 49.73%. I_3,3(1:4-dioxan) requires In, 15.10; I, 50.13%]: this decomposes without melting 103° to (ii) InI_3,(1:4-dioxan), dissociation pressure 0.2 cm at 39.1°. [Found: , 19.60; I, 65.16%. InI_3,(1:4-dioxan) requires In, 19.66; I, 65.24%.] This complex elted at about 234° with considerable charring which began to be evident at 220°. irect solubility measurements gave:

$t°$	*Mole %*	*s (g InI_3/100 g dioxan)*
12.0	1.67	9.5
19.0	2.02	11.6
26.1	2.50	14.5
32.6	3.06	17.8

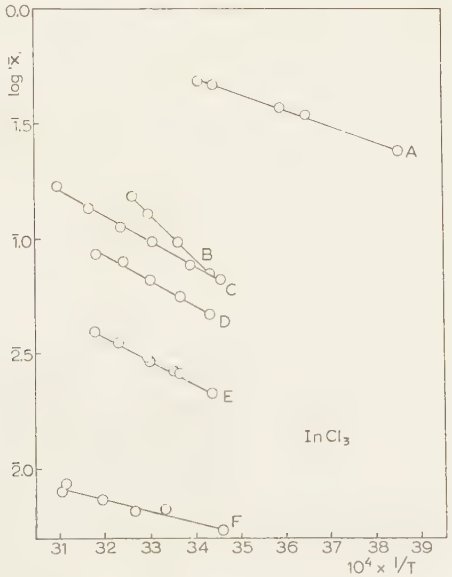

ig. 1. $InCl_3$: (A) diethyl ether; (B) tetrahydrofuran; (C) 1:4-dioxan; (D) di-isoamyl ether; (E) di-*n*-butyl ether; (F) di-isopropyl ether.

The solubilities over temperature ranges between about —40°C and +60°C of the three trihalides in a number of ethers — expressed for uniformity in terms of log mole fraction ($\bar{x}_1$) of halide, though the solid phase in different systems may be the crystalline halide itself or a complex — are plotted against $1/T$ in Figs. 1 and 2.

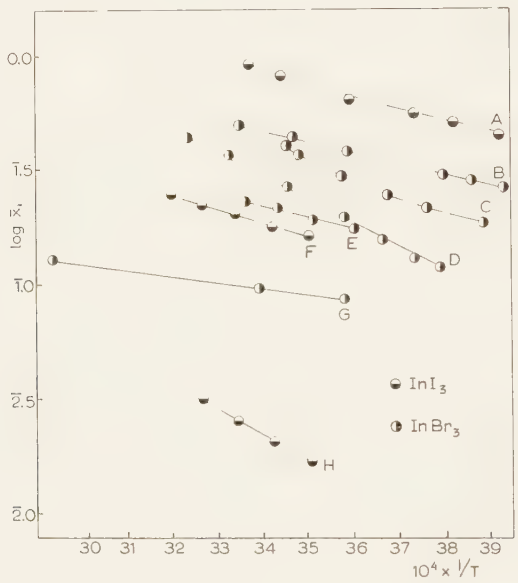

Fig. 2. $InBr_3$: (B) diethyl ether; (C) di-*n*-butyl ether; (D) di-isopropyl ether; (E) tetrahydrofuran; (G) 1:4-dioxan.
InI_3: (A) diethyl ether; (F) tetrahydrofuran; (H) 1:4-dioxan.

With the object of providing a comparison between the heats of formation of these complexes and of those formed with the trihalides of other members of this group, a number of calorimetric measurements were made of heats of dissolution of the halides in diethyl ether. These were carried out by dissolution of the samples in 300 ml pure dry ether, contained in an unsilvered Dewar vessel immersed in a water thermostat and securely sealed against ingress of moisture or evaporation by a brass cover which carried the stirrer, auxiliary heater and thermometer. The temperature was measured (to within $\pm$ 0.002°) by a Stantel Type F.2311/300 thermistor, previously calibrated; and the heat capacity of the calorimeter and its contents by means of an auxiliary heating coil, in the usual manner. Specimens were contained in fragile glass ampoules attached to the lower end of the stirrer by thin platinum wires looped round the lower blades. The glass stirrer was held by a teflon block to the brass stirring shaft, which in turn passed through a bearing packed with teflon turnings and through a spring-loaded radial ball-bearing, surmounted by a thrust bearing This enabled the stirrer to be depressed whilst in motion and crush the ampoule against a pointed glass anvil at the bottom of the reaction vessel. Since it was found to be impracticable to introduce 300 ml of dry ether into the reaction vessel without introduction of traces of moisture, and since even rigorous purification may fail to remove all traces of impurities which might react with the halides, inconsistent results were at first ob-

tained. A procedure of "pre-treatment" of the ether with the appropriate halide was then adopted. This consisted in the addition of about 1 g of the halide to the ether immediately before closing the vessel by the lid with its attachments. The supernatant air was then displaced by dry nitrogen, the vessel finally sealed and the ether stirred until a steady state was reached, before depressing the stirrer to fracture the ampoule. In this way 3 or 4 values for each system, generally consistent to within 0.05 kcal.mole^{-1}, were obtained. We also carried out, for comparison, similar measurements with aluminium trichloride, tribromide and triiodide. For some of these we are indebted to the help given by R. H. BEAUMONT[8] and A. H. COWLEY[9].

Since the slowness of dissolution of indium trichloride in ether precludes the use of simple direct measurement of the heat of solution in ether, recourse was made to an indirect method. This consisted of the measurement of the heats of dissolution in water, of anhydrous trichloride, and of a concentrated ether solution of the ether complex, due allowance being made for the heat of solution of the combined and excess ether in the water. Since, in order to obtain the heats of formation of these complexes in the reactions

$$MCl_{3(c)} + x(C_2H_5)_2O_{(l)} \rightarrow MCl_3,x(C_2H_5)_2O_{(c)}$$

the heat of dissolution of the complex in excess ether is also required, samples of the complex were prepared and the heats of dissolution obtained in the same manner. In this way the values given in Table II were obtained.

TABLE II

Parent halide		*Complex*		
	Heat of solution in diethyl ether ΔH (kcal.mole^{-1})		*Heat of solution in diethyl ether ΔH (kcal.mole^{-1})*	*Heat of formation ΔH (kcal.mole^{-1})*
$AlCl_3$	—13.6[8]	$AlCl_3,Et_2O$	+2.3	—15.9
$AlBr_3$	—20.9[9]	$AlBr_3,Et_2O$	+2.0	—22.9
AlI_3	—18.5[9]	AlI_3,Et_2O	+3.2	—21.7
$InCl_3$	— 9.4	$InCl_3,2Et_2O$	+1.6	—11.0
$InBr_3$	— 8.4	$InBr_3,2Et_2O$	+0.1	— 8.5
InI_3	— 8.0[8]	InI_3,Et_2O	—2.4	— 5.6

All the three indium trihalides dissolve exothermically in ether but with a smaller heat of reaction than the aluminium halides. All the complexes, with the exception of $InI_3,(C_2H_5)_2O$ dissolve with absorption of heat. The exceptional position of indium triiodide in this respect suggests that, although only one solid complex was observed under the conditions of the experiment, further solvation may occur in solution, with possibly the formation of a di-etherate stable only at much lower temperatures. Additional evidence in this direction is provided by the apparent molecular weights of the complex in solution, which were from 11% to 14% higher than would be ex-

pected on the basis of $InI_3,(C_2H_5)_2O$; also, the solubility of this complex, like those of all the other complexes, increased with rise of temperature.

DISCUSSION

Three outstanding features emerge from these results. Firstly there is the extreme slowness of dissolution of indium trichloride, even in ethers with which it forms stable complexes and in which the ultimate solubility is high. Secondly, it may be observed that 1:2 complexes greatly preponderate and in the third place the character of the ethers themselves, probably their steric configuration, affects the formation of complexes.

We believe that the slowness of dissolution of indium trichloride is to be associated with its structure. In the solid state it forms an ionic layer-lattice[10] with the extraordinarily high melting point of $586 \pm 3°$[11], which is much the highest of any trichloride, tribromide or triiodide of aluminium, gallium or indium, and is then only attained under increased pressure. The indium trichloride melt is still largely ionic in character, as is shown by its equivalent conductivity at the melting point of 14.7 $ohm^{-1}cm^{-1}$, which is about 11% of that of molten sodium chloride[12] and about 10^6 times that of molten aluminium chloride. Melting is accompanied by a very large decrease in density. There are no data for the density of the solid near the melting point but since the estimated increase in molar volume from —273° to 25° is only from 63.2 to 63.9[13] one would not expect a volume change of a mass of solid indium trichloride from room temperature to melting to be more than a few percent. Yet the volume of molten indium trichloride is some 65% greater ($d_4^{591} = 2.11$) than that of the same mass of solid ($d^{25} = 3.45$) at 25° with a further increase to 75% with a rise of temperature of only 69°, an abnormal expansion commented upon by KLEMM. There also occurs over a range of temperature of 100° above the melting point, a 12.5% decrease in conductivity which must be associated with a further shift of the equilibrium towards the molecular structure, produced therefore from the ionic with an absorption of heat.

Indium trichloride vaporises as single molecules. Between 606° and 850° the vapour density corresponds to the formula $InCl_3$[14]. The existence of double molecules In_2Cl_6, corresponding to those formed by aluminium or gallium trichlorides has never been proved, since at temperatures at which they might be stable the vapour pressure is too small to measure.

Since numerous estimates, in the present work, of the molecular weights of the complexes in ether solution, by the depression of the vapour pressures of the solutions, show that they are mostly present as *e.g.* $InCl_3,2(C_2H_5)_2O$, their formation must involve a re-organization of the acceptor compound in the direction $InCl_3$ (ionic solid) → $InCl_3$ (molecules), which is an endothermic process. This process in an ether must necessarily occur on the surface of the solid halide, and the slow formation of the very soluble complex is probably due to the presence of this heat of ionic → molecular transition as an activation energy.

What the magnitude of the energy of this ionic-molecular transition is we do not know, but evidently it becomes greater as the radius of the positive ion increases and less with increase in radius of the halogen, as one would expect. All the trihalides of boron are molecular. Aluminium trichloride in the solid state is ionic, but even the heat of fusion is sufficient to bring about a conversion to the molecular

structure as is also the case with gallium trichloride, tribromide and triiodide[15].

The triiodide is the only indium trihalide which is reported to have molecular structure in the solid state[10]. It melts to a liquid with an equivalent conductance only about 15% that of molten indium trichloride and which *increases* with rise of temperature. We find accordingly that indium trichloride dissolves much more slowly in any ether than does the triiodide.

Indium tribromide, which gives a melt with a conductance (6.4 $ohm^{-1}cm^{-1}$) only a little less than half that of indium trichloride[12] and which also has a negative temperature coefficient, though smaller by a factor of 17, is in an intermediate position.

It may be observed that of the 25 complexes described above, 18 are formed by the combination of two molecules of ether with one of InX_3. This raises the question whether the indium possesses a co-ordinate covalence of five, in these complexes, involving a 5*d* orbital, or whether the indium is quadricovalent, utilizing only 6*s* and 6*p* orbitals, with one chlorine pushed out as an ion, *e.g.*: $[InCl_2,2Et_2O]^+Cl^-$. The evidence up to the present does not seem clear-cut, one way or the other, and further work is required. Indium trichloride has a small conductivity in ethyl ether solution which is about 10^{-3} that of the equivalent conductance of tetra-amylammonium picrate in the same solvent[16], and the specific conductance of molten $InBr_3,2(C_2H_5)_2O$ at 25° was $5.7 \cdot 10^{-5}$ $ohm^{-1}cm^{-1}$. On the other hand, the fairly low melting points of most of these complexes suggest a covalent structure. The matter could be determined by an X-ray analysis of the structures, which seems feasible since several can easily be grown as well-defined single crystals.

Considerable variation was found in the complexing power of the different ethers, especially with indium trichloride. In the case of isopropyl-, *n*-butyl, or isoamyl-ethers no complex formation was observed and equilibrium was established only slowly, over 3 days. The solubilities in these ethers was very much less than in other ethers in which complex formation occurred. This may be due to steric hindrance since these ethers all have large volumes of rotation. It is significant that when the intramolecular rotation is restricted complex formation is facilitated. Thus, at a given temperature, the complex $InCl_3$,2-tetrahydrofuran has a much lower dissociation pressure than $InCl_3$,2(diethyl-ether) and whereas no complex was formed between this halide and di-isopropyl ether, stable 1 : 2 complexes were formed with 2-methyltetrahydrofuran and 2–5 dimethyltetrahydrofuran.

REFERENCES

1 W. C. SCHUMB AND H. I. CRANE, *J. Am. Chem. Soc.*, 60 (1938) 306.
2 I. A. SHEKA, *J. Gen. Chem. U.S.S.R.*, 26 (1956) 25.
3 G. UREN, *M. Sc. Thesis*, Manchester, 1948.
4 W. REPPE, *Ann.*, 596 (1955) 110.
5 A. H. COWLEY, F. FAIRBROTHER AND N. SCOTT, *J. Chem. Soc.*, (1958) 3133.
6 F. FAIRBROTHER, N. SCOTT AND H. PROPHET, *J. Chem. Soc.*, (1956) 1164.
7 F. ENSSLIN AND O. LESSMANN, *Z. anorg. Chem.*, 254 (1947) 92.
8 R. H. BEAUMONT, *M. Sc. Thesis*, Manchester, 1957.
9 A. H. COWLEY, *M. Sc. Thesis*, Manchester, 1956.
10 Ref. GMELIN'S *Handbuch der anorganischen Chemie*, Verlag Chemie, G.m.b.H., Weinheim, 8th ed., Vol. 37, p. 80.
11 W. KLEMM, *Z. anorg. Chem.*, 152 (1926) 254.
12 H. BILTZ AND W. KLEMM, *Z. anorg. Chem.*, 152 (1926) 267.
13 W. KLEMM AND F. DIERKS, *Z. anorg. Chem.*, 219 (1934) 44.
14 L. F. NILSON AND O. PETTERSON, *Z. phys. Chem.*, 2 (1888) 661.
15 N. N. GREENWOOD AND I. J. WORRALL, *J. Inorg. & Nuclear Chem.*, 3 (1956) 357.
16 P. WALDEN, *Z. Phys. Chem.*, (A), 147 (1930) 1.

Book Review

Tantalum and Niobium, by G. L. MILLER, Butterworths Scientific Publications, London; 120s (Academic Press Inc., New York; $21.00.); 767 pages.

Tantalum and Niobium are expensive metals, but they have valuable properties and their use is expanding. The appearance of this book is therefore opportune, and since it covers both the chemistry and metallurgy of these metals in considerable detail, it should prove equally attractive to those concerned with their production, their compounds, and their industrial applications.

In its twelve chapters the book deals with practically every aspect of these metals, commencing with their occurrence, consumption and extraction, and concluding with their properties, alloying propensities and compounds. Chemical analyses, metallographic techniques suitable for tantalum and its alloys, and thermodynamic data for some compounds of both metals are given in Appendices. The book is written in a masterly fashion, with great attention to detail. On reading it, one is soon convinced that the author is an authority on his subject, and despite the misgivings which he expresses in his preface, it is difficult to suggest any directions in which the planning of the book could have been improved or the subject matter expanded. Efforts have obviously been made to ensure the inclusion of the latest available information, and this is particularly apparent in the lengthy chapter on binary alloys, but every chapter is almost a book in itself, and as an illustration that dealing with the consolidation of these metals covers the subject from the earliest work on sintering to the latest developments in arc- and electron-beam melting. Equally informative is the chapter on physical and structural properties, while that dealing with corrosion by chemicals, gases, and liquid metals is most comprehensive.

The book is a worthy addition to the series of monographs on the Metallurgy of the Rarer Metals. It is adequately illustrated and indexed, and contains extensive references to published work at the end of each chapter. It can confidently be recommended to all those seeking the latest information on tantalum and niobium, and should serve as a standard work of reference for some time to come.

J.W.C.

J. Less-Common Metals, 2 (1960) 64

CONTENTS

The constitution of thorium-zirconium alloys containing more than 15% zirconium and the effect of some third elements on the stability of body-centred-cubic phase in these alloys
by J. R. MURRAY (Harwell) 1

Ordering in Co-NiPt alloys
by J. C. WOOLLEY AND B. BATES (Nottingham) 11

The equilibrium diagram of the system molybdenum–rhodium
by E. ANDERSON AND W. HUME-ROTHERY (Oxford) 19

The preparation of high purity vanadium pentoxide by a chlorination procedure
by R. E. MCCARLEY AND J. W. RODDY (Ames, Iowa) 29

Some observations on decomposition of metastable beta-phase in titanium–chromium alloys
by K. A. GROSS AND I. R. LAMBORN (Maribyrnong, Australia) 36

Relationships between impact and low-strain-rate hydrogen embrittlement of titanium alloys
by D. N. WILLIAMS AND R. I. JAFFEE (Ohio) 42

Complex compounds of indium trihalides. Part 1. Ether complexes
by F. FAIRBROTHER, N. FLITCROFT AND H. PROPHET (Manchester) 49

Book Review 64

All rights reserved

ELSEVIER PUBLISHING COMPANY, AMSTERDAM

Printed in The Netherlands by

NEDERLANDSE BOEKDRUK INRICHTING N.V., 'S-HERTOGENBOSCH

ELSEVIER'S

SCIENTIFIC JOURNALS

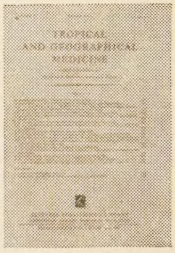

ANALYTICA CHIMICA ACTA

BIOCHIMICA ET BIOPHYSICA ACTA

JOURNAL OF CHROMATOGRAPHY

CLINICA CHIMICA ACTA

ICSU REVIEW

TROPICAL AND
GEOGRAPHICAL MEDICINE

EPILEPSIA

JOURNAL OF
ELECTROANALYTICAL CHEMISTRY

WEAR - USURE - VERSCHLEISS

Specimen copies are available

ELSEVIER PUBLISHING COMPANY
110-112 SPUISTRAAT — AMSTERDAM — THE NETHERLANDS